



HAL
open science

Closed-form solutions for the elastic–plastic buckling design of shell structures under external pressure

Van-Dong Do, Philippe Le Grogneq, Philippe Rohart

► **To cite this version:**

Van-Dong Do, Philippe Le Grogneq, Philippe Rohart. Closed-form solutions for the elastic–plastic buckling design of shell structures under external pressure. *European Journal of Mechanics - A/Solids*, 2023, 98, pp.104861. 10.1016/j.euromechsol.2022.104861 . hal-03970484

HAL Id: hal-03970484

<https://ensta-bretagne.hal.science/hal-03970484>

Submitted on 11 Jul 2024

HAL is a multi-disciplinary open access archive for the deposit and dissemination of scientific research documents, whether they are published or not. The documents may come from teaching and research institutions in France or abroad, or from public or private research centers.

L'archive ouverte pluridisciplinaire **HAL**, est destinée au dépôt et à la diffusion de documents scientifiques de niveau recherche, publiés ou non, émanant des établissements d'enseignement et de recherche français ou étrangers, des laboratoires publics ou privés.

Closed-form solutions for the elastic-plastic buckling design of shell structures under external pressure

Van-Dong Do^a, Philippe Le Grogne^{a,*}, Philippe Rohart^b

^a*ENSTA Bretagne, UMR CNRS 6027, IRDL, F-29200 Brest, France*

^b*CETIM, Centre Technique des Industries Mécaniques, 5 avenue Félix Louat - BP 80067, F-60304 Senlis Cedex, France*

Abstract

This paper deals with the elastoplastic buckling analysis of shell geometries traditionally encountered in pressure vessels subjected to external pressure loading. The objective is to propose in a unified way original analytical closed-form solutions giving rise to reliable results, with a good accuracy and a wide range of applications in a straightforward and low time-consuming way, for efficient dimensioning purposes. The present study is based on the plastic bifurcation theory, classically used in the context of conservative systems, where additional terms are incorporated here due to the follower external pressure acting normally to the deformed surface of the shell still after buckling. Cylindrical shells are first considered, which certainly represent the most fundamental components of pressure vessels in practice. Owing to the external pressure also acting on the closure ends of a cylinder, the influence of the induced axial compression is investigated thereafter. It appears to be non-negligible for short cylinders in elasticity and it becomes very significant in the case of plastic buckling. Then, closed-form solutions for the critical external pressure of a complete sphere are also obtained, both in elasticity and plasticity. Finally, all these new closed-form solutions are validated against reference numerical results obtained through finite element computations, and compared to current design rules.

Keywords: Pressure vessels, elastic-plastic buckling, pressure end thrust, analytical solutions, numerical validation, design rules

*Corresponding author.

Email address: philippe.le_grogne@ensta-bretagne.fr (Philippe Le Grogne)

1. Introduction

Shell structures are widely used in a variety of industrial applications such as buildings, transportation facilities, deep-diving submarines and pressure vessels, thanks to the economic benefits of such thin structures. In the particular case of pressure vessels, the buckling phenomenon (or geometric instability) represents one of the main failure modes encountered in practice, due to the thinness of the structures and the predominant compressive stresses currently observed under standard loads such as external pressure. Therefore, a thorough buckling analysis of such structures is generally required in standard design procedures.

Many shell buckling problems have been studied in the literature so far, involving various geometries such as cylinders, spheres, ellipsoids, cones or any combination of them. Among the loadings which typically give rise to geometric instabilities, the external pressure has clearly a prominent place. The vast majority of these papers deal with elastic buckling analyses and several analytical solutions are already available in such conditions. Most investigations are concerned with cylindrical shells which are certainly the most essential components in pressure vessels. Energy methods are the most popular approaches used to determine the critical buckling pressure and Bryan [1] was the first to derive an analytical solution of the elastic critical buckling pressure of long tubes under external pressure, using such an energy method. More recently, the elastic buckling of long cylindrical shells under uniform external pressure was still the topic of several analytical studies. One can mention Paimushin [2], Xue [3], Salahshour and Fallah [4], among others. Southwell [5] as for him considered the case of short cylinders under uniform external pressure. Yamaki [6] thoroughly investigated the elastic stability problem of circular cylindrical shells. He analyzed both the buckling and post-buckling behavior from a theoretical and experimental point of view, considering several geometric configurations and many loading cases among which the external pressure. However, no exact closed-form expression was provided for the critical pressure, but instead, only approximate empirical formulae. Grigolyuk and Kabanov [7] derived an analytical expression of the critical pressure for thin cylindrical shells with simply-supported end conditions. Papadakis [8] proposed a new analytical expression of the critical pressure in the case of thick cylindrical shells under external pressure, including the effects of transverse shear in the analysis. Nguyen et al. [9] also investigated analytically the elastic buckling of cylindrical shells under

external pressure, considering a variable thickness. Finally, one can mention Basaglia et al. [10] who were interested in the use of the Generalized Beam Theory (GBT) for the elastic buckling analysis of steel cylindrical shells under combinations of axial compression and external pressure.

Numerous studies have also been conducted on the buckling behavior of spherical shells under external pressure, since this fundamental geometry is also frequently encountered in practice. Zoelly [11] was the first to derive an analytical solution for the critical external pressure of elastic buckling for a perfect spherical shell. Hutchinson [12, 13] analyzed the post-buckling behavior of spherical shells under external pressure within the context of Koiter's general theory and showed the significant imperfection sensitivity of such a problem, even in elasticity. Palusamy and Lind [14] developed a consistent theory for the limit analysis of spherical shells under radial pressure. Sato et al. [15] investigated the axisymmetric buckling response of spherical shells filled with an elastic medium subjected to external pressure.

Besides, pressure vessels (especially cylinders) generally include closure ends of various shapes, which may be hemispherical, ellipsoidal, torispherical or toriconical. Also, some transitions of conical shape are sometimes encountered between different cylindrical parts of pressure equipments. All these ends and connecting zones have also to sustain reliably extreme design loads, and require thus a detailed buckling analysis. However, only few studies deal with such shell geometries. One can mention, for instance, the review paper from Krivoschapko [16] dealing with static, dynamic and stability analyses of complete ellipsoidal shells (and also ellipsoidal heads and bottoms), specially focusing on ellipsoids of revolution and building applications. A few approximate solutions for the critical external pressure are particularly listed with their respective domain of validity. Otherwise, one only finds some numerical or experimental studies concerning the buckling of ellipsoidal structures, such as the finite element analysis of super ellipsoidal shells under uniform pressure [17] and the recent non-linear buckling analysis of a semi-elliptical dome [18]. Dealing with conical shells, one can cite Sharghi et al. [19] who analyzed the buckling of laminated conical shells under axial compression, using trigonometric and power series, and Chung [20] who handled the more general case of composite conical shells under combined axial compression, external pressure and bending.

The buckling problem is much more difficult to analyze when considering thicker structures, for which plasticity may occur before buckling. Shanley [21] was probably the first to derive the so-called tangent modulus criti-

cal load for a discrete model, which corresponds to the minimum possible plastic buckling load at which the structure may buckle in practice. Later, a few results have been obtained concerning columns, plates or shells under various loadings and boundary conditions. Among others, Becque [22] investigated recently the inelastic buckling of thin-walled columns in an analytical way, accounting for flexural but also torsional modes. Much earlier, empirical formulae were already proposed for the plastic buckling loads of simply-supported sandwich plates under uniaxial compression, arising from simplifying assumptions [23]. The existence of continua of bifurcation points in plastic buckling problems was emphasized by Cimetière [24] in the case of compressed rectangular plates. As regards shell plastic buckling analyses, the case of axially compressed circular cylindrical shells was certainly one of the most considered, which is further limited to axisymmetric modes. In this context, one can mention the pioneering works of Batterman [25, 26] who derived first adequate formulae for the critical axial compressive stress in a cylindrical shell with various boundary conditions.

The plastic buckling of a cylindrical shell under external pressure was far less commonly studied than the elastic case. The pioneering works on this subject are certainly due to Chakrabarty [27, 28]. He examined first the general conditions under which bifurcation may occur in a shell under pressure loading beyond the elastic limit, and considered then the particular case of cylindrical shells subjected to external fluid pressure. More recently, Takla investigated numerically both material and geometric instability phenomena (such as necking, bulging, column buckling and section collapse) in elastoplastic cylindrical shells under internal/external pressure and/or axial tension/compression [29–32]. One can also find some rare experimental studies on this subject, such as the one from Zhu et al. [33], which considers a very specific constitutive law and clamped ends. Besides, unlike the case of cylindrical shells, to the best authors' knowledge, there is no plastic buckling analysis of spherical shells in the literature, at least analytically speaking.

When dealing with shell buckling, large discrepancies are often observed between theoretical predictions and experimental results, which may be due to unavoidable imperfections in experiments, among other things. This imperfection sensitivity was discussed by many authors, such as Hutchinson [34] in his asymptotic analysis of plastic post-buckling. As far as plastic buckling is concerned, different critical values may be obtained, depending on the retained plasticity theory, and the strong discrepancy between the results provided by the flow and deformation theories has been observed by

many authors. Among others, Liu [35] analyzed the imperfection sensitivity of uniaxially compressed plates by means of finite element computations, using both flow and deformation theories for comparison purposes. Ore and Durban [36] also confronted the two theories by deriving two series of semi-analytical values for the critical load of a cylinder under axial compression under various boundary conditions. In most cases, it turns out that the flow theory largely overpredicts the experimental critical values, whereas the deformation theory gives rise to predictions in much better agreement, although the latter does not include the elastic unloading possibility. This major issue is known as the plastic buckling paradox, and it has been partially explained by the fact that the flow theory induces an elastic shear modulus at onset of buckling. It is particularly detrimental to problems of torsional buckling of beams, among others, for which the torsional stiffness is thus not affected by the plasticity occurring during the uniaxial compression, as emphasized in [22]. Otherwise, it is now well established that the use of the flow theory (namely tangent moduli) is a better option. For example, many years ago, Neale [37] carried out a theoretical analysis of the influence of imperfections on the plastic buckling of rectangular plates, using a Reissner-type variational principle. He showed the close agreement between the results deriving from the flow theory and the deformation theory (and thus also with experimental data), provided that imperfections were conveniently accounted for in the formulation.

Finally, let us mention the existence of many practical methodologies that have been developed for the buckling design of pressure vessels. These methods are generally assembled in standards and codes such as the ASME Boiler and Pressure Vessel Code (BPVC) [38] or the French CODAP [39]. The design rules are either analytical (based on abacuses or formulae), but limited thus to a certain range of validity, or in the form of general recommendations [40] for performing finite element analyses in the presence of geometric and/or material non-linearities and imperfections [41].

This paper deals with the buckling analysis of shell structures under external pressure. In view of the preceding literature review, it is specially devoted to the search for new analytical solutions for the elastic but, above all, plastic buckling critical values. In the longer term, the aim of this contribution is to enrich and simplify simultaneously the current calculation rules in standard codes with new explicit solutions, enabling thus an ever more efficient dimensioning with both a better accuracy and a wider range of applications. The present study is based on the 3D plastic bifurcation theory,

assuming the J_2 flow theory of plasticity with the von Mises yield criterion and a linear isotropic hardening. The 3D results are then particularized to the case of a thin shell, considering the plane stress hypothesis and assuming a pre-critical biaxial stress state. The so-called shallow shell theory is retained so as to describe the kinematics in a simple way. A particular attention is given to the follower external pressure, which is supposed to remain normal to the shell surface during all the deformation process (even in the post-buckling range). Owing to this non-conservative loading, the classical bifurcation equation is slightly modified and the critical pressure is found to be possibly different from the corresponding critical value obtained when a dead load is considered. Finally, the previous formulation is applied to the cases of cylindrical and spherical shells, which represent the most encountered shapes in practical pressure vessels and enable one to obtain closed-form solutions. An axial compressive force is added to the external pressure in the case of cylindrical shells so as to take into account the well-known pressure end thrust.

The main contribution of the present work is to propose a generic method, based on the so-called bifurcation equation, which is able to provide in a straightforward way both elastic and plastic critical buckling loads of arbitrary shells under compressive loadings. In particular, it will be shown that the shallow shell theory is a good compromise in that it allows for simple and yet reliable closed-form expressions of the sought critical loads. The following applications concern the two fundamental geometries of the cylinder and the sphere, and they are focused on external pressure loading (possibly combined with longitudinal compression in the case of cylindrical shells). However, the generality of the method augurs well for future applications dealing with other geometries and/or other loading conditions. In addition to the method itself, some original results are established and validated, which may serve as an alternative to current empirical design rules.

Section 2 summarizes first the main features of the plastic bifurcation theory and presents the general formulation of the problem. Then, the two case studies are detailed in Section 3, leading to closed-form solutions for the critical pressure, both in elasticity and plasticity (the latter being mostly original). In Section 4, numerical finite element computations are performed, using Abaqus software, and the analytical and numerical results are discussed and compared to each other, for validation purposes. Last, in Section 5, a short comparison between the new formulae obtained in this paper and the solutions derived from standard codes (CODAP/ASME) gives an insight of

the relevance of such new closed-form solutions, especially in plasticity.

2. General formulation

2.1. 3D plastic bifurcation theory

The subsequent developments are based on the theory of plastic bifurcation, the main issues of which having already been presented in detail in [42]. The most significant and useful results will be recalled here for the sake of completeness.

The following elastoplastic buckling analyses are carried out, as usual, by means of a total Lagrangian formulation, within the framework of the standard generalized materials theory [43, 44]. As pre-critical deformations are supposed to remain moderate in the present study, one can make use of the Green strain tensor \mathbf{E} which will be split additively into its elastic and plastic parts, respectively \mathbf{E}^e and \mathbf{E}^p , leading next to expressions similar to those obtained classically in small strains [45, 46].

The elastic response of the material is assumed to be isotropic and is therefore represented by the Saint-Venant-Kirchhoff law, involving the fourth-order elasticity tensor \mathbf{D} whose components in an orthonormal basis are $D_{ijkl} = \lambda\delta_{ij}\delta_{kl} + \mu(\delta_{ik}\delta_{jl} + \delta_{il}\delta_{kj})$, where δ_{ij} is the Kronecker symbol and λ and μ are the Lamé constants. Use will also be made of Young's modulus E and Poisson's ratio ν which are related to λ and μ by $\lambda = \frac{E\nu}{(1+\nu)(1-2\nu)}$ and $\mu = \frac{E}{2(1+\nu)}$.

In the plastic regime, the plastic threshold is defined by the von Mises yield function with a linear isotropic hardening:

$$f(\boldsymbol{\Sigma}, A) = \sqrt{\frac{3}{2}\boldsymbol{\Sigma}^d : \boldsymbol{\Sigma}^d} - \sigma_0 - A \quad A = Hp_{eq} \quad (1)$$

where $\boldsymbol{\Sigma}^d$ denotes the deviatoric part of the second Kirchhoff stress tensor $\boldsymbol{\Sigma}$ and p_{eq} the equivalent plastic strain. σ_0 is the initial yield stress and H represents the (constant) hardening modulus.

The material tangent elastoplastic tensor writes then:

$$\mathbf{D}^p = \frac{\partial \boldsymbol{\Sigma}}{\partial \mathbf{E}} = \mathbf{D} - \frac{\mathbf{D} : \frac{\partial f}{\partial \boldsymbol{\Sigma}} \otimes \frac{\partial f}{\partial \boldsymbol{\Sigma}} : \mathbf{D}}{H + \frac{\partial f}{\partial \boldsymbol{\Sigma}} : \mathbf{D} : \frac{\partial f}{\partial \boldsymbol{\Sigma}}} \quad (2)$$

and the nominal tangent elastoplastic tensor can finally be expressed as follows:

$$\mathbf{K}^p = \frac{\partial \boldsymbol{\Pi}}{\partial \mathbf{F}} = \mathbf{F} \cdot \frac{\partial \boldsymbol{\Sigma}}{\partial \mathbf{E}} \cdot \mathbf{F}^T + (\mathbb{I} \cdot \boldsymbol{\Sigma})^T \quad (3)$$

where \mathbf{F} is the deformation gradient, $\mathbf{\Pi} = \mathbf{F}\cdot\boldsymbol{\Sigma}$ the first Kirchhoff stress tensor, \mathbb{I} stands for the fourth-order unit tensor ($\mathbb{I}_{ijkl} = \delta_{il}\delta_{kj}$) and the superscript T means the transposition of a second-order tensor or the major transposition of a fourth-order tensor defined by $(A^T)_{ijkl} = A_{klji}$.

In the case of small pre-critical deformations, the nominal tangent tensor can be reduced to:

$$\mathbf{K}^p \approx \mathbf{D}^p + (\mathbb{I}\cdot\boldsymbol{\Sigma})^T \quad (4)$$

where $(\mathbb{I}\cdot\boldsymbol{\Sigma})^T$ depends on the stress state and thus on the loading factor (say ξ) which will act further as the bifurcation parameter.

Now, let us assume that (i) the buckling phenomenon occurs in the plastic zone (the whole solid is assumed to be plastified on the fundamental branch at critical time) and that (ii) the bifurcation takes place at the tangent modulus critical load (with incipient unloading). It implies that the yield stress σ_0 is small enough for the plastic strains to appear before buckling. In these conditions, the critical loading ξ_c and the corresponding buckling mode \mathbf{X} of an arbitrary 3D body Ω can be obtained by solving the following bifurcation equation [47, 48]:

$$\forall \delta\mathbf{u}, \quad \int_{\Omega} \nabla^T \delta\mathbf{u} : \mathbf{K}^p(\xi_c) : \nabla\mathbf{X} \, d\Omega = 0 \quad (5)$$

where $\delta\mathbf{u}$ can be considered as a test function or, more physically, as the virtual variation of the unknown displacement field \mathbf{u} . Such an equation has been initially derived in the context of conservative systems. As will be seen in a later section, additional terms will be included in the formulation so as to take into account the follower nature of the external pressure in the present study.

2.2. Biaxial stress state

In this section, the expressions of the elastoplastic tangent tensors \mathbf{D}^p and \mathbf{K}^p will be explicated in the special case of a uniform biaxial stress state, which is consistent with the pre-buckling stress distributions observed in the following analyses.

Let $(\mathbf{e}_1, \mathbf{e}_2, \mathbf{e}_3)$ be a fixed orthonormal basis. Owing to the small strain assumption, the second Kirchhoff stress tensor coincides with the first Kirchhoff stress tensor which is supposed to be written in this basis as follows:

$$\boldsymbol{\Sigma} \approx \mathbf{\Pi} = -\eta\xi\mathbf{e}_1 \otimes \mathbf{e}_1 - \xi\mathbf{e}_2 \otimes \mathbf{e}_2 = \begin{bmatrix} -\eta\xi & 0 & 0 \\ 0 & -\xi & 0 \\ 0 & 0 & 0 \end{bmatrix} \quad (\xi > 0, \eta \in \mathbb{R}) \quad (6)$$

where the tensor expression and its matrix representation in the basis $(\mathbf{e}_1, \mathbf{e}_2, \mathbf{e}_3)$ have been put together for the sake of brevity. The loading level is reflected by the value of parameter ξ and the scalar coefficient η represents the ratio between the stress in the \mathbf{e}_1 -direction and that in the \mathbf{e}_2 -direction. One has thus a compressive stress in the \mathbf{e}_2 -direction, whereas a compressive or tensile stress may be observed in the \mathbf{e}_1 -direction, depending on the sign of η . Hence, the material tangent elastoplastic tensor of Equation (2) becomes:

$$\mathbf{D}^p = \mathbf{D} - \frac{\mu^2}{(H+3\mu)(1-\eta+\eta^2)} [\eta(\mathbf{I} - 3\mathbf{e}_1 \otimes \mathbf{e}_1) + \mathbf{I} - 3\mathbf{e}_2 \otimes \mathbf{e}_2] \otimes [\eta(\mathbf{I} - 3\mathbf{e}_1 \otimes \mathbf{e}_1) + \mathbf{I} - 3\mathbf{e}_2 \otimes \mathbf{e}_2] \quad (7)$$

where \mathbf{I} is the second-order unit tensor.

The components of \mathbf{D}^p in the orthonormal basis $(\mathbf{e}_1, \mathbf{e}_2, \mathbf{e}_3)$ are:

$$\begin{aligned} D_{1111}^p &= \lambda + 2\mu - \frac{\mu^2(1-2\eta)^2}{(H+3\mu)(1-\eta+\eta^2)} \\ D_{2222}^p &= \lambda + 2\mu - \frac{\mu^2(2-\eta)^2}{(H+3\mu)(1-\eta+\eta^2)} \\ D_{3333}^p &= \lambda + 2\mu - \frac{\mu^2(1+\eta)^2}{(H+3\mu)(1-\eta+\eta^2)} \\ D_{1122}^p &= \lambda + \frac{\mu^2(1-2\eta)(2-\eta)}{(H+3\mu)(1-\eta+\eta^2)} \\ D_{1133}^p &= \lambda - \frac{\mu^2(1-2\eta)(1+\eta)}{(H+3\mu)(1-\eta+\eta^2)} \\ D_{2233}^p &= \lambda + \frac{\mu^2(2-\eta)(1+\eta)}{(H+3\mu)(1-\eta+\eta^2)} \\ D_{1212}^p &= D_{1313}^p = D_{2323}^p = \mu \end{aligned} \quad (8)$$

The other components are either zero or derived from Equation (8) using both major and minor symmetries of tensor \mathbf{D}^p ($D_{ijkl}^p = D_{klij}^p = D_{jikl}^p = D_{ijlk}^p$).

The nominal tangent elastoplastic tensor of Equation (3) then writes:

$$\mathbf{K}^p = \mathbf{D}^p - \eta\xi\mathbf{e}_i \otimes \mathbf{e}_1 \otimes \mathbf{e}_1 \otimes \mathbf{e}_i - \xi\mathbf{e}_i \otimes \mathbf{e}_2 \otimes \mathbf{e}_2 \otimes \mathbf{e}_i \quad (9)$$

which is independent of the spatial coordinates (implicit summations are made on repeated indices).

Furthermore, when dealing with two-dimensional models like plates or shells, an ad hoc assumption has to be added in order to enforce some specific stress state in the body. Namely, the normal material stress is assumed to be zero: $\Sigma_{33} = 0$. Taking into account this assumption leads one to recast the 3D constitutive law and to replace tensor \mathbf{D}^p in Equation (9) with a reduced one denoted by \mathbf{C}^p , whose components in the orthonormal basis $(\mathbf{e}_1, \mathbf{e}_2, \mathbf{e}_3)$

are:

$$C_{ijkl}^p = D_{ijkl}^p - \frac{D_{ij33}^p D_{33kl}^p}{D_{3333}^p} \quad (i, j) \neq (3, 3), (k, l) \neq (3, 3) \quad (10)$$

Tensor \mathbf{C}^p has the major and both minor symmetries and the following notations will be further used for brevity:

$$\begin{aligned} \alpha = C_{2222}^p &= E \frac{1+4\eta(\eta-1)+3\frac{E_T}{E}}{(5-4\nu)(1+\eta^2)-2(4-5\nu)\eta-(1-2\nu)[(1-2\nu)(1+\eta^2)-2(2-\nu)\eta]\frac{E_T}{E}} \\ \beta = C_{1122}^p &= E \frac{2-5\eta+2\eta^2-[2(1-2\nu)(1+\eta^2)-(5-4\nu)\eta]\frac{E_T}{E}}{(5-4\nu)(1+\eta^2)-2(4-5\nu)\eta-(1-2\nu)[(1-2\nu)(1+\eta^2)-2(2-\nu)\eta]\frac{E_T}{E}} \\ \gamma = C_{1111}^p &= E \frac{(2-\eta)^2+3\eta^2\frac{E_T}{E}}{(5-4\nu)(1+\eta^2)-2(4-5\nu)\eta-(1-2\nu)[(1-2\nu)(1+\eta^2)-2(2-\nu)\eta]\frac{E_T}{E}} \end{aligned} \quad (11)$$

where the tangent modulus E_T is related to the Young's modulus E and the isotropic hardening modulus H by $\frac{1}{E_T} = \frac{1}{E} + \frac{1}{H}$.

Finally, in a biaxial stress state and under the plane stress condition, the bifurcation equation (5) writes:

$$\forall \delta \mathbf{u}, \quad \int_{\Omega} \nabla^T \delta \mathbf{u} : (\mathbf{C}^p - \eta \xi_c \mathbf{e}_i \otimes \mathbf{e}_1 \otimes \mathbf{e}_1 \otimes \mathbf{e}_i - \xi_c \mathbf{e}_i \otimes \mathbf{e}_2 \otimes \mathbf{e}_2 \otimes \mathbf{e}_i) : \nabla \mathbf{X} \, d\Omega = 0 \quad (12)$$

2.3. Follower external pressure

The cylindrical and spherical shells further analyzed will be mainly subjected to an external pressure which naturally always acts perpendicularly to the shell surface. This follower nature of the load makes the problem no more conservative and additional terms are needed in the bifurcation equation (12) in order to take into account the supplementary work done by the external pressure on the deformed shell surface. This problem has been extensively described by Paimushin [2, 49, 50] in the context of elastic buckling analyses of cylindrical shells under external pressure and it was also discussed in detail in [10]. The main issue is that the buckling pressure may highly depend on whether one considers a dead or follower load.

Let again $(\mathbf{e}_1, \mathbf{e}_2, \mathbf{e}_3)$ be a (local) orthonormal basis with \mathbf{e}_1 and \mathbf{e}_2 being tangent to the undeformed surface of the shell at the considered point and \mathbf{e}_3 the corresponding normal unit vector. The displacement vector of a point on the mid-surface of the shell can be expressed in this basis as follows:

$$\mathbf{U} = U\mathbf{e}_1 + V\mathbf{e}_2 + W\mathbf{e}_3 \quad (13)$$

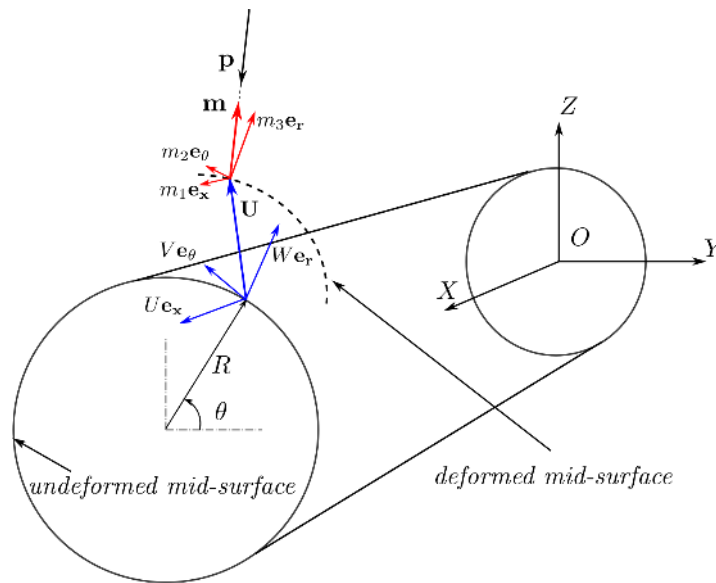


Figure 1: Circular cylindrical shell under follower external pressure

and as can the virtual displacement field. The example of a cylindrical shell is illustrated in Figure 1 with the use of a cylindrical coordinate system.

When considering a conservative dead pressure, the load vector simply writes:

$$\mathbf{p} = -p\mathbf{e}_3 \quad (14)$$

as pressure is invariably a radially inward force in the direction of the undeformed normal to the surface, and the associated external work is as follows:

$$W_{ext}^{dead} = \int_S \mathbf{p} \cdot \delta \mathbf{U} \, dS = - \int_S p \delta W \, dS \quad (15)$$

where S stands for the whole surface of the shell.

The classical bifurcation equation (5) turns out to be the difference between two rate equilibrium equations, one for the bifurcated solution and the other one for the fundamental solution. Since the external work term appearing in these two equations is similar in the conservative case (it does not depend on the rates considered), it does not occur anymore in the final bifurcation equation (the pressure is only taken into account through the nominal tangent tensor).

Conversely, in the case of a follower external pressure, the load vector becomes:

$$\mathbf{p} = -p\mathbf{m} = -p(m_1\mathbf{e}_1 + m_2\mathbf{e}_2 + m_3\mathbf{e}_3) \quad (16)$$

where \mathbf{m} is the modified normal (see Figure 1), namely the outward unit vector perpendicular to the actual deformed surface, and the associated external work is as follows:

$$W_{ext}^{follower} = \int_S \mathbf{p} \cdot \delta \mathbf{U} \, dS = - \int_S p(m_1\delta U + m_2\delta V + m_3\delta W) \, dS \quad (17)$$

In the general case, the expressions of m_1 , m_2 and m_3 (which depend on the geometry and the kinematics of the shell) are highly non-linear. If it is assumed that the rotations are small, some simplifications can be made. m_3 can be taken as equal to 1, in such a way that the corresponding term in the external work will be discarded as in the conservative case. As for m_1 and m_2 , only the linear non-conservative terms will be retained, which will be specified in the sequel. In the end, only the path-dependent external work must be deduced from the original bifurcation equation, and the new equation to be solved will thus take the following form:

$$\forall \delta \mathbf{u}, \quad \int_{\Omega} \nabla^T \delta \mathbf{u} : (\mathbf{C}^p - \eta \xi_c \mathbf{e}_i \otimes \mathbf{e}_1 \otimes \mathbf{e}_1 \otimes \mathbf{e}_i - \xi_c \mathbf{e}_i \otimes \mathbf{e}_2 \otimes \mathbf{e}_2 \otimes \mathbf{e}_i) : \nabla \mathbf{X} \, d\Omega + \int_S p_c(m_1\delta U + m_2\delta V) \, dS = 0 \quad (18)$$

where p_c stands for the critical external pressure. Thereafter, in each successive application, the bifurcation parameter ξ and thus the corresponding critical value ξ_c will be adequately expressed in terms of the external pressure p and the associated critical value p_c , respectively. The value of coefficient η will also depend on the considered problem.

2.4. Shallow shell theory

In the following applications, it will be supposed that the wavelengths of the buckling modes are small when compared to the smallest radius of curvature of the shell. In such conditions, the shallow shell theory can be used, which can be viewed as a flat plate theory including corrective terms so as to take into account the curvatures of the shell. In practice, one considers the plane tangent to the shell surface at a current point, and cartesian coordinates x and y are defined in this plane in such a way that the projection of the lines along the shell with principal radii of curvature on the tangent

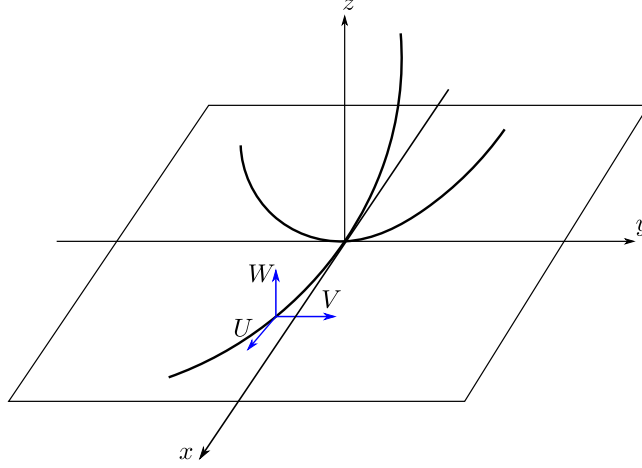


Figure 2: Shallow shell theory: use of cartesian coordinates in the tangent plane

plane coincide with \mathbf{x} and \mathbf{y} axes. A third coordinate z is then defined in the direction normal to the shell (see Figure 2).

In concrete terms, the displacement \mathbf{u} of an arbitrary point of the shell can be initially viewed as a function of the three displacements $U(x, y)$, $V(x, y)$ and $W(x, y)$ along \mathbf{x} , \mathbf{y} and \mathbf{z} axes, respectively, of its projection onto the mid-surface, according to the classical thin plate kinematics:

$$\mathbf{u} = \begin{pmatrix} U - zW_{,x} \\ V - zW_{,y} \\ W \end{pmatrix} \quad (19)$$

However, the gradient (or deformation) terms do not only derive from the displacement field above, but also include complementary terms stemming from the curvatures of the shell. Without going into details, the following simplified results can be used, assuming that the in-plane displacements U and V are considerably smaller than the out-of-plane displacement W (see [51] for more information). The displacement gradient, which appears in the bifurcation equation (18), turns out to be equal to:

$$\nabla \mathbf{u} = \begin{bmatrix} U_{,x} - zW_{,xx} - \frac{W}{R_x} & U_{,y} - zW_{,xy} & -W_{,x} \\ V_{,x} - zW_{,xy} & V_{,y} - zW_{,yy} - \frac{W}{R_y} & -W_{,y} \\ W_{,x} & W_{,y} & 0 \end{bmatrix} \quad (20)$$

where R_x and R_y are the algebraic principle radii of curvature of the shell along \mathbf{x} and \mathbf{y} axes, respectively.

3. Analytical solutions

3.1. Cylindrical shells

3.1.1. External pressure

Let us consider first the problem of a simply-supported cylindrical shell under external pressure. These boundary conditions enable one to obtain closed-form solutions and correspond at best to the real conditions in the presence of closure ends. The cylindrical shell is defined in the reference configuration by its length L , its average radius R and thickness $t \ll R$ (see Figure 3). The external pressure p gives rise to a uniaxial compressive hoop stress in the circumferential direction $-\xi = -\frac{pR}{t}$. The preceding general biaxial formulation in Section 2.2 can be used here once η is set to zero.

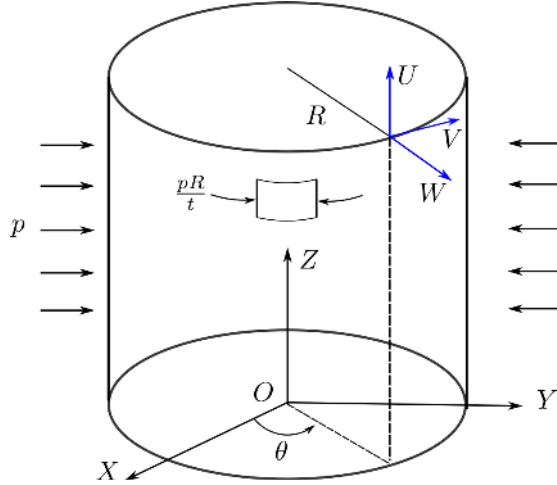


Figure 3: Cylindrical shell under external pressure

Within the context of the shallow shell theory, \mathbf{x} and \mathbf{y} axes are chosen as being respectively along the longitudinal and circumferential directions, so that R_x is infinite and $R_y = -R$ (this radius of curvature is negative since the radial displacement is directed towards the outside of the cylinder).

The gradient of the bifurcation mode can thus be written as follows:

$$\nabla \mathbf{X} = \begin{bmatrix} \mathcal{U}_{,x} - z\mathcal{W}_{,xx} & \mathcal{U}_{,y} - z\mathcal{W}_{,xy} & -\mathcal{W}_{,x} \\ \mathcal{V}_{,x} - z\mathcal{W}_{,xy} & \mathcal{V}_{,y} - z\mathcal{W}_{,yy} + \frac{\mathcal{W}}{R} & -\mathcal{W}_{,y} \\ \mathcal{W}_{,x} & \mathcal{W}_{,y} & 0 \end{bmatrix} \quad (21)$$

where \mathcal{U} , \mathcal{V} and \mathcal{W} stand for the three displacement components of the buckling mode \mathbf{X} along \mathbf{x} , \mathbf{y} and \mathbf{z} axes, respectively. The gradient of the displacement variation $\delta\mathbf{u}$ takes a similar form.

According to this kinematics, the in-plane components of the normal vector to the deformed mid-surface of the cylindrical shell are $m_1 = -\mathcal{W}_{,x}$ and $m_2 = -\mathcal{W}_{,y}$, as soon as only linear terms are retained.

With all these considerations, the bifurcation equation (18) can be explicitated and solved. For this purpose, the tensor product $\nabla^T \delta\mathbf{u} : \mathbf{K}^p(\xi_c) : \nabla\mathbf{X}$ is performed and first integrated in the shell thickness (from $z = -\frac{t}{2}$ to $\frac{t}{2}$). Then, the whole equation is adequately integrated by parts with respect to x and y , giving rise to the three following local partial differential equations:

$$\begin{cases} \gamma t \mathcal{U}_{,xx} + (\beta + \mu) t \mathcal{V}_{,xy} + \left(\frac{\beta t}{R} + p\right) \mathcal{W}_{,x} + (\mu t - pR) \mathcal{U}_{,yy} = 0 \\ (\alpha t - pR) \mathcal{V}_{,yy} + (\beta + \mu) t \mathcal{U}_{,xy} + \frac{\alpha t}{R} \mathcal{W}_{,y} + \mu t \mathcal{V}_{,xx} = 0 \\ \frac{\gamma t^3}{12} \mathcal{W}_{,xxxx} + \left(\frac{(\beta+2\mu)t^3}{6} - \frac{pRt^2}{12}\right) \mathcal{W}_{,xxyy} + \left(\frac{\alpha t^3}{12} - \frac{pRt^2}{12}\right) \mathcal{W}_{,yyyy} \\ + \left(\frac{\alpha t}{R} - p\right) \mathcal{V}_{,y} + \frac{\beta t}{R} \mathcal{U}_{,x} + \left(\frac{\alpha t}{R^2} - \frac{p}{R}\right) \mathcal{W} + pR \mathcal{W}_{,yy} = 0 \end{cases} \quad (22)$$

together with the corresponding natural boundary conditions, which will be specified later. Presupposing that pre-critical deformations are small, a classical assumption is to neglect the stresses in relation to elastic moduli (and elastoplastic ones, by extension). In practice, it results in $\frac{pR}{t} \ll \alpha, \beta, \gamma, \mu$, and it allows us to remove all the pressure terms between parentheses, so that only one pressure term remains at the end of the third equation. By doing so, the additional pressure terms originating from the follower nature of the external pressure eventually turn out to disappear. It means that, with such a shallow shell formulation, only one solution is expected, regardless of whether one considers a follower or dead external pressure. It can be noticed that, when using a more classical approach involving the more convenient cylindrical coordinate system or in numerical analyses, one obtains two different expressions or values of the critical pressure, depending on its dead or follower nature. It will be shown here that the single solution arising from the use of shallow shell theory will be unexpectedly in better agreement with the follower critical pressure.

As the special practical case of simply-supported end conditions has been retained, the following displacement boundary conditions hold:

$$\begin{cases} \mathcal{V}(0, y) = \mathcal{V}(L, y) = 0 \\ \mathcal{W}(0, y) = \mathcal{W}(L, y) = 0 \end{cases} \quad (23)$$

This particular choice to set the circumferential displacement to zero and not the longitudinal one enables one to get a simple explicit expression for the critical buckling mode, as will be seen later. One must then verify the following natural boundary conditions, deriving from the previous integration by parts, that can be identified as the expression of a null axial normal force and a null bending moment per unit length at both ends:

$$\begin{cases} \gamma t \mathcal{U}_{,x}(0, y) + \beta t \mathcal{V}_{,y}(0, y) + \frac{\beta t}{R} \mathcal{W}(0, y) = 0 \\ \gamma t \mathcal{U}_{,x}(L, y) + \beta t \mathcal{V}_{,y}(L, y) + \frac{\beta t}{R} \mathcal{W}(L, y) = 0 \\ \frac{\gamma t^3}{12} \mathcal{W}_{,xx}(0, y) + \frac{\beta t^3}{12} \mathcal{W}_{,yy}(0, y) = 0 \\ \frac{\gamma t^3}{12} \mathcal{W}_{,xx}(L, y) + \frac{\beta t^3}{12} \mathcal{W}_{,yy}(L, y) = 0 \end{cases} \quad (24)$$

The bifurcation mode satisfying all these boundary conditions may be taken in the following form:

$$\begin{cases} \mathcal{U} = \mathcal{U}_0 \cos\left(\frac{m\pi x}{L}\right) \cos\left(\frac{ny}{R}\right) \\ \mathcal{V} = \mathcal{V}_0 \sin\left(\frac{m\pi x}{L}\right) \sin\left(\frac{ny}{R}\right) \\ \mathcal{W} = \mathcal{W}_0 \sin\left(\frac{m\pi x}{L}\right) \cos\left(\frac{ny}{R}\right) \end{cases} \quad (25)$$

By inserting these expressions for the components of the buckling mode in Equation (22), one obtains a linear system of homogeneous equations, whose determinant must vanish in order to get a non-trivial solution. Solving this determinant leads to the following general expression for the critical pressure:

$$\begin{aligned} p_e^{cyl} = & \left(t \left[\alpha^2 \mu^2 n^8 L^8 + \alpha R^2 t^2 m^2 n^6 L^6 \pi^2 (\alpha \gamma - \beta^2 + 4\mu^2) \right. \right. \\ & + R^4 m^4 \pi^4 L^4 \left[12\mu R^2 (\alpha \gamma - \beta^2) + n^4 t^2 (-8\mu^2 \beta + \mu(6\alpha \gamma - 8\beta^2) + 2\beta(\alpha \gamma - \beta^2)) \right] \\ & \left. \left. + \gamma R^6 t^2 m^6 n^2 \pi^6 L^2 (\alpha \gamma - \beta^2 + 4\mu^2) + \mu \gamma^2 m^8 t^2 \pi^8 R^8 \right] \right) \\ & / \left(12R^3 L^4 n^2 \left[\alpha \mu n^4 L^4 + R^2 m^2 n^2 \pi^2 L^2 (\alpha \gamma - \beta^2 - 2\beta \mu) + \gamma \mu \pi^4 R^4 m^4 \right] \right) \end{aligned} \quad (26)$$

In the case where buckling occurs in the elastic regime ($E_T = E$), one can use the elastic expressions of the reduced moduli: $\alpha = \gamma = \frac{E}{1-\nu^2}$ and $\beta = \frac{E\nu}{1-\nu^2}$. The elastic critical pressure writes then:

$$p_e^{cyl} = \frac{Et}{Rn^2} \frac{\left(\frac{m\pi R}{L}\right)^4}{\left[\left(\frac{m\pi R}{L}\right)^2 + n^2\right]^2} + \frac{D}{R^3 n^2} \left[\left(\frac{m\pi R}{L}\right)^2 + n^2 \right]^2 \quad (27)$$

where $D = \frac{Et^3}{12(1-\nu^2)}$ is the classical elastic bending stiffness.

This problem of elastic buckling of a cylindrical shell under external pressure has been widely investigated in the literature, and it has led to several expressions for the critical pressure, according to the underlying assumptions, whose validity may depend on the geometric configuration (length-to-radius or thickness-to-radius ratios, among other things). The present closed-form solution takes a very simple form and it will be shown in the subsequent validation section that it is valid for a large range of geometries. This formula has already been derived in [7], but in a different way. In Equation (27), the critical pressure depends on the circumferential wave number n and the longitudinal half-wave number m , which have to be adequately identified so as to find the minimum critical pressure, which alone is of practical interest.

When considering the elastoplastic expressions for the reduced moduli α , β and γ in Equation (11), one obtains the analytical solution of the plastic buckling critical pressure:

$$\begin{aligned}
p_p^{cyl} = & - \left(Et \left[t^2 n^8 L^8 (E + 3E_T)^2 (1 + \nu) - 8\pi^2 t^2 m^2 n^6 R^2 L^6 (E + 3E_T) \right. \right. \\
& \left. \left. (E(\nu - \frac{5}{4}) - 3E_T(\nu + \frac{1}{4})) + 24\pi^4 m^4 R^4 L^4 \left(t^2 n^4 (E^2(\nu - 2) \right. \right. \right. \\
& \left. \left. \left. - 3E_T E(\nu - 3) + 6E_T^2(\nu - \frac{1}{2})) - 8R^2 E_T (1 + \nu) (E(\nu - \frac{5}{4}) + E_T(\nu - \frac{1}{2})^2) \right) \right. \right. \\
& \left. \left. \left. - 32\pi^6 t^2 m^6 n^2 E R^6 L^2 (E(\nu - \frac{5}{4}) - 3E_T(\nu + \frac{1}{4})) + 16\pi^8 R^8 t^2 E^2 m^8 (1 + \nu) \right] \right) \\
& / \left(48L^4 n^2 R^3 (1 + \nu) \left[E(\nu - \frac{5}{4}) + E_T(\nu - \frac{1}{2})^2 \right] \right. \\
& \left. (n^4 L^4 (E + 3E_T) - 4R^2 m^2 n^2 \pi^2 L^2 (E - 3E_T) + 4E\pi^4 R^4 m^4) \right)
\end{aligned} \tag{28}$$

Equation (28) is an original and quite long but closed-form expression of the critical pressure of a cylindrical shell in the plastic regime. Again, the wave numbers will be chosen appropriately so as to deal further with the minimum buckling pressure. This formula will be validated in Section 4.

3.1.2. External pressure and axial compression

In practice, cylindrical pressure vessels are closed with top and bottom ends, in such a way that the external pressure acting on these ends gives rise to a given axial compression stress in the cylindrical shell, independent of their shape (see Figure 4). This axial stress is half of the circumferential stress, namely it is equal to $-\frac{pR}{2t}$. In these real conditions, the cylindrical shell undergoes a biaxial stress state. Nevertheless, it can be shown that the buckling phenomenon is still mainly due to the circumferential compressive

stresses, but that the critical pressure may slightly change due to the non-negligible axial compressive stresses.

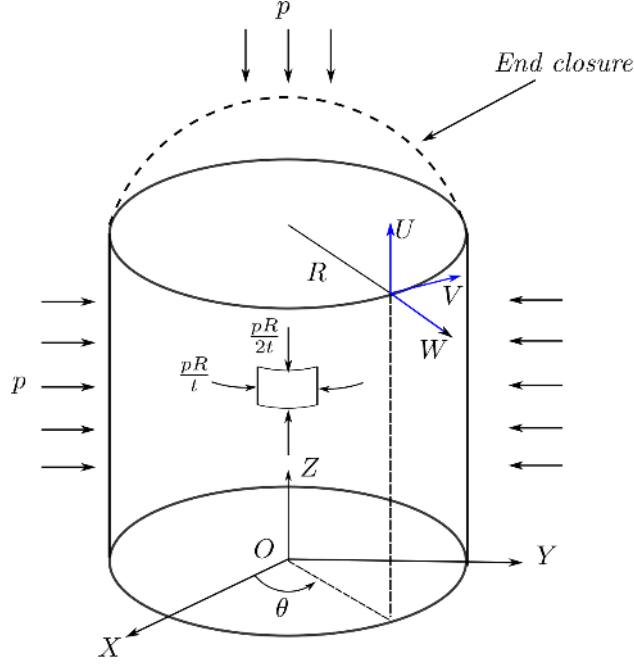


Figure 4: Cylindrical shell under external pressure and axial compression

In this section, one considers thus a cylinder subjected to a biaxial compressive stress state, which amounts to taking $\xi = \frac{pR}{t}$ and $\eta = \frac{1}{2}$ in the preceding general formulation. Let us mention that the reduced moduli will also change (at least in plasticity), due to this new biaxial stress state. Without going into details, by taking into account the pressure end thrust, the three local buckling equations become:

$$\begin{cases} \gamma t \mathcal{U}_{,xx} + (\beta + \mu) t \mathcal{V}_{,xy} + \frac{\beta t}{R} \mathcal{W}_{,x} + \mu t \mathcal{U}_{,yy} = 0 \\ \alpha t \mathcal{V}_{,yy} + (\beta + \mu) t \mathcal{U}_{,xy} + \frac{\alpha t}{R} \mathcal{W}_{,y} + \mu t \mathcal{V}_{,xx} = 0 \\ \frac{\gamma t^3}{12} \mathcal{W}_{,xxxx} + \frac{(\beta + 2\mu)t^3}{6} \mathcal{W}_{,xxyy} + \frac{\alpha t^3}{12} \mathcal{W}_{,yyyy} + \frac{\alpha t}{R} \mathcal{V}_{,y} + \frac{\beta t}{R} \mathcal{U}_{,x} \\ + \frac{\alpha t}{R^2} \mathcal{W} + \frac{pR}{2} \mathcal{W}_{,xx} + pR \mathcal{W}_{,yy} = 0 \end{cases} \quad (29)$$

where some pressure terms have already been discarded for the same reasons as above.

The same kinematic and natural boundary conditions as before apply at both ends of the cylindrical shell, and the same general expressions (25) can

be used for the modal components. Finally, one obtains a new expression for the critical external pressure:

$$\begin{aligned}
p_c^{cyl-end} = & \left(t \left[\alpha^2 \mu t^2 n^8 L^8 + \alpha R^2 t^2 m^2 n^6 L^6 \pi^2 (\alpha \gamma - \beta^2 + 4\mu^2) + R^4 m^4 \pi^4 L^4 \right. \right. \\
& \left. \left[12\mu R^2 (\alpha \gamma - \beta^2) + n^4 t^2 (-8\mu^2 \beta + \mu(6\alpha \gamma - 8\beta^2) + 2\beta(\alpha \gamma - \beta^2)) \right] \right. \\
& \left. + \gamma R^6 t^2 m^6 n^2 \pi^6 L^2 (\alpha \gamma - \beta^2 + 4\mu^2) + \mu \gamma^2 m^8 t^2 \pi^8 R^8 \right] \\
& / \left((6R^5 L^2 \pi^2 m^2 + 12R^3 L^4 n^2) \left[\alpha \mu n^4 L^4 + R^2 m^2 n^2 \pi^2 L^2 \right. \right. \\
& \left. \left. (\alpha \gamma - \beta^2 - 2\beta \mu) + \gamma \mu \pi^4 R^4 m^4 \right] \right)
\end{aligned} \tag{30}$$

A new analytical solution is thus obtained for the elastic critical pressure:

$$p_e^{cyl-end} = \left(\frac{Et}{Rn^2} \frac{\left(\frac{m\pi R}{L}\right)^4}{\left[\left(\frac{m\pi R}{L}\right)^2 + n^2\right]^2} + \frac{D}{R^3 n^2} \left[\left(\frac{m\pi R}{L}\right)^2 + n^2\right]^2 \right) \frac{n^2}{n^2 + \frac{1}{2}\left(\frac{m\pi R}{L}\right)^2} \tag{31}$$

In Equation (31), the term between parentheses corresponds to the elastic critical pressure calculated without considering the pressure end thrust. The new solution is therefore lower than the previous one, the axial compression being detrimental to the current buckling phenomenon.

A new original formula is then obtained for the plastic buckling critical pressure, also taking into consideration the new expressions of α , β and γ in the present biaxial stress state:

$$\begin{aligned}
p_p^{cyl-end} = & \left(Et \left[\frac{1}{2} t^2 \pi^8 m^8 R^8 (E + \frac{E_T}{3})^2 (1 + \nu) + \pi^4 m^4 R^6 L^2 \right. \right. \\
& \left(E_T^2 \left[\frac{8}{9} n^2 t^2 m^2 \pi^2 (\nu + \frac{5}{8}) - \frac{32}{3} L^2 (\nu - \frac{1}{2}) (\nu + 1) (\nu + \frac{1}{2}) \right] \right. \\
& \left. + 8EE_T \left[\frac{1}{3} n^2 t^2 m^2 \pi^2 (\nu + \frac{3}{4}) + L^2 (1 + \nu) \right] + E^2 \pi^2 m^2 t^2 n^2 \right) \\
& \left. + \frac{4}{3} E_T L^4 n^4 t^2 \pi^4 m^4 R^4 [E_T (3\nu + 1) + E(\nu + 3)] \right. \\
& \left. + \frac{4}{3} E_T n^6 \pi^2 t^2 L^6 m^2 R^2 \left[\frac{1}{3} E_T (8\nu + 5) + E \right] + \frac{8}{9} E_T^2 n^8 L^8 t^2 (1 + \nu) \right] \\
& / \left(6L^2 R^3 \left(\frac{1}{2} \pi^2 R^2 m^2 + L^2 n^2 \right) \left[E + \frac{1}{3} E_T (1 - 4\nu^2) \right] (\nu + 1) \right. \\
& \left. [m^4 \pi^4 R^4 (E + \frac{1}{3} E_T) + \frac{8}{3} \pi^2 R^2 E_T m^2 n^2 L^2 + \frac{4}{3} E_T n^4 L^4] \right)
\end{aligned} \tag{32}$$

3.2. Spherical shells under external pressure

Let us now consider the case of a spherical shell under external pressure. The sphere is defined in the reference configuration by its average radius R

and thickness $t \ll R$ (see Figure 5). The external pressure gives rise here to a compressive equi-biaxial stress state, which amounts to taking $\xi = \frac{pR}{2t}$ and $\eta = 1$ in the preceding formulation.

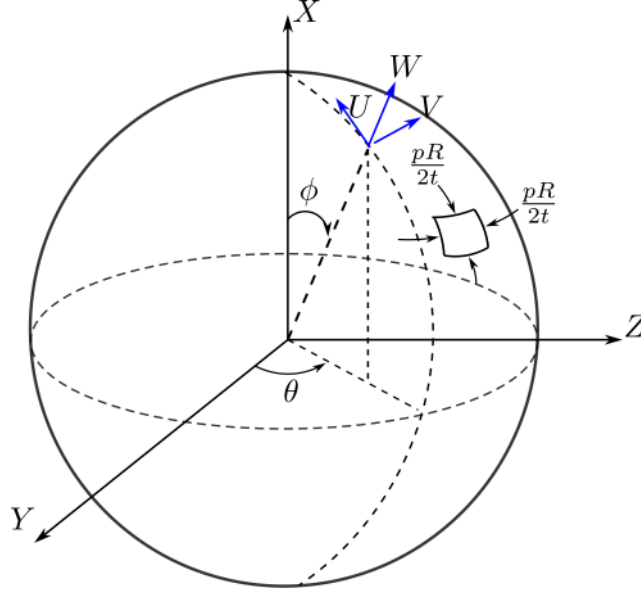


Figure 5: Spherical shell under external pressure

Within the context of the shallow shell theory, \mathbf{x} and \mathbf{y} axes are chosen as being along two perpendicular great circles (or orthodromes) of the sphere, so that $R_x = R_y = -R$.

The gradient of the bifurcation mode can thus be written as follows:

$$\nabla \mathbf{X} = \begin{bmatrix} \mathcal{U}_{,x} - z\mathcal{W}_{,xx} + \frac{\mathcal{W}}{R} & \mathcal{U}_{,y} - z\mathcal{W}_{,xy} & -\mathcal{W}_{,x} \\ \mathcal{V}_{,x} - z\mathcal{W}_{,xy} & \mathcal{V}_{,y} - z\mathcal{W}_{,yy} + \frac{\mathcal{W}}{R} & -\mathcal{W}_{,y} \\ \mathcal{W}_{,x} & \mathcal{W}_{,y} & 0 \end{bmatrix} \quad (33)$$

and the gradient of the displacement variation $\delta \mathbf{u}$ takes a similar form.

According to this kinematics, the in-plane components of the normal vector to the deformed mid-surface of the spherical shell are $m_1 = -\mathcal{W}_{,x}$ and $m_2 = -\mathcal{W}_{,y}$, like in the previous case of a cylindrical shell.

Then, after integration in the shell thickness and integration by parts

with respect to x and y , the following buckling equations are derived:

$$\begin{cases} \left(\alpha t - \frac{pR}{2} \right) \mathcal{U}_{,xx} + (\beta + \mu)t \mathcal{V}_{,xy} + \left(\frac{(\alpha+\beta)t}{R} + \frac{p}{2} \right) \mathcal{W}_{,x} + \left(\mu t - \frac{pR}{2} \right) \mathcal{U}_{,yy} = 0 \\ \left(\alpha t - \frac{pR}{2} \right) \mathcal{V}_{,yy} + (\beta + \mu)t \mathcal{U}_{,xy} + \left(\frac{(\alpha+\beta)t}{R} + \frac{p}{2} \right) \mathcal{W}_{,y} + \left(\mu t - \frac{pR}{2} \right) \mathcal{V}_{,xx} = 0 \\ \left(\frac{\alpha t^3}{12} - \frac{pRt^2}{24} \right) \mathcal{W}_{,xxxx} + \left(\frac{(\beta+2\mu)t^3}{6} - \frac{pRt^2}{12} \right) \mathcal{W}_{,xxyy} + \left(\frac{\alpha t^3}{12} - \frac{pRt^2}{24} \right) \mathcal{W}_{,yyyy} \\ + \left(\frac{(\alpha+\beta)t}{R} - \frac{p}{2} \right) \mathcal{V}_{,y} + \left(\frac{(\alpha+\beta)t}{R} - \frac{p}{2} \right) \mathcal{U}_{,x} + \left(\frac{2(\alpha+\beta)t}{R^2} - \frac{p}{R} \right) \mathcal{W} + \frac{pR}{2} \mathcal{W}_{,xx} + \frac{pR}{2} \mathcal{W}_{,yy} = 0 \end{cases} \quad (34)$$

where γ has been replaced by α since these two coefficients are equal, both in elasticity and plasticity, due to the equi-biaxial stress state. By removing all the negligible pressure terms in Equation (34), one obtains the following simplified system:

$$\begin{cases} \alpha t \mathcal{U}_{,xx} + (\beta + \mu)t \mathcal{V}_{,xy} + \frac{(\alpha+\beta)t}{R} \mathcal{W}_{,x} + \mu t \mathcal{U}_{,yy} = 0 \\ \alpha t \mathcal{V}_{,yy} + (\beta + \mu)t \mathcal{U}_{,xy} + \frac{(\alpha+\beta)t}{R} \mathcal{W}_{,y} + \mu t \mathcal{V}_{,xx} = 0 \\ \frac{\alpha t^3}{12} \mathcal{W}_{,xxxx} + \frac{(\beta+2\mu)t^3}{6} \mathcal{W}_{,xxyy} + \frac{\alpha t^3}{12} \mathcal{W}_{,yyyy} \\ + \frac{(\alpha+\beta)t}{R} \mathcal{V}_{,y} + \frac{(\alpha+\beta)t}{R} \mathcal{U}_{,x} + \frac{2(\alpha+\beta)t}{R^2} \mathcal{W} + \frac{pR}{2} \mathcal{W}_{,xx} + \frac{pR}{2} \mathcal{W}_{,yy} = 0 \end{cases} \quad (35)$$

where all the follower terms related to the external pressure do not appear again.

Owing to the periodicity conditions inherent in the spherical nature of the shell, the bifurcation mode may take the following form:

$$\begin{cases} \mathcal{U} = \mathcal{U}_0 \sin\left(\frac{k_x x}{R}\right) \cos\left(\frac{k_y y}{R}\right) \\ \mathcal{V} = \mathcal{V}_0 \cos\left(\frac{k_x x}{R}\right) \sin\left(\frac{k_y y}{R}\right) \\ \mathcal{W} = \mathcal{W}_0 \cos\left(\frac{k_x x}{R}\right) \cos\left(\frac{k_y y}{R}\right) \end{cases} \quad (36)$$

where k_x and k_y are the wave numbers of the solution, respectively in the x and y directions. By introducing the expressions above into the system of partial differential equations (35) and solving the appropriate determinant, one obtains again a general formula for the plastic buckling critical pressure of a spherical shell:

$$p_p^{sph} = \frac{Et \left[k_{xy}^2 t^2 (E^2 + 6EE_T + 9E_T^2) + 96(1 - \nu - 2\nu^2)E_T^2 R^2 + 96EE_T(1 + \nu)R^2 \right]}{12k_{xy}(E + 3E_T)(1 + \nu) \left((1 - 2\nu)E_T + E \right) R^3} \quad (37)$$

where $k_{xy} = k_x^2 + k_y^2$. As a result of this specific combination of the two independent wave numbers in the general solution, it appears that at each critical pressure (related to a specific value of k_{xy}) correspond many multiple modes with as many pairs of wave numbers. In practice, k_x and k_y (and thus k_{xy}) are sufficiently high so that the minimum critical pressure can be obtained with a very good approximation by minimizing expression (37) with respect to k_{xy} considered as a real number (even though it is actually an integer). After derivation of the expression of p_p^{sph} as a function of k_{xy} , one obtains the minimum plastic buckling pressure:

$$p_p^{sph} = \frac{2}{3} \frac{\sqrt{6EE_T}}{\sqrt{E_T(\nu+1)(-2E_T\nu + E + E_T)}} \left(\frac{t}{R}\right)^2 \quad (38)$$

which corresponds to buckling modes with any combination of wave numbers k_x and k_y that satisfies:

$$k_x^2 + k_y^2 = k_{xy} = \frac{4R\sqrt{-12E_T^2\nu^2 + 6EE_T\nu - 6E_T^2\nu + 6EE_T + 6E_T^2}}{t(E + 3E_T)} \quad (39)$$

To the best of the authors' knowledge, the closed-form solution (38) is the first expression in the literature of the plastic buckling critical value of a spherical shell under external pressure. This formula is quite simple and gives rise, by taking $E_T = E$, to the well-known elastic value initially derived by Zoelly [11]:

$$p_e^{sph} = \frac{2E}{\sqrt{3(1-\nu^2)}} \left(\frac{t}{R}\right)^2 \quad (40)$$

4. Numerical applications and finite element validation

4.1. Numerical modeling using Abaqus software

In this section, the previous closed-form solutions will be validated against numerical results obtained through finite element computations using Abaqus software. In elasticity, linearized buckling analyses can be performed but, in plasticity, incremental calculations are needed so as to take into account the material non-linearities. In practice, such computations are called Geometrically and Materially Non-linear Analyses with Imperfections (GMNIA). Use is made of arc-length approaches (Riks method) so as to deal with non-monotonous equilibrium curves. In addition, imperfections are possibly introduced (when necessary) so as to trigger the buckling phenomenon and

follow the post-critical equilibrium path. Among a number of alternatives, an initial geometric imperfection is preferred (when needed), in the shape of the sought first buckling mode, which can be considered as the worst imperfection type. This initial imperfection is included after a preliminary linearized buckling analysis, with an optimal amplitude (the minimum value leading to effective buckling). The resulting equilibrium curve obtained with such a computation is supposed to be a slightly degenerated curve, when compared to the idealized curve stemming from the perfect structure, and it classically displays a limit point coinciding or almost coinciding with the sought bifurcation point (at least in the two present configurations). In the following validation sections, the analytical critical pressures will thus be confronted to the limit admissible pressures arising from the numerical equilibrium curves. The immediate post-critical deformed shapes will also be plotted so as to identify the relevant first mode and compare it with the analytical wave numbers.

Dealing with the finite element method, a shell finite element model is retained, made of eight-node (quadratic) elements with five degrees-of-freedom per node and reduced integration (S8R5 elements in Abaqus). A structured mesh is built (as far as possible) and a mesh convergence study is performed in each case. A parametric model has been developed so as to adjust the proper geometric dimensions and material properties. Finally, the desired boundary conditions are enforced (some of which to prevent from possible rigid modes) and an external pressure is applied all over the shell structure.

4.2. Cylindrical shells

The case of an elastic cylindrical shell is first considered. Owing to the symmetry of the expected buckling modes, only a quarter of the cylinder is modeled (half of the length and half of the circumference), which considerably reduces the computation times. The geometric parameters and elastic properties are listed in Tables 1 and 2, respectively. When applying the external pressure on the shell, two options are available (namely the choice between a dead or follower pressure). These two assumptions conduce to somewhat different critical values in the present case of a cylindrical shell. Here, a follower pressure is naturally retained, as it corresponds to more realistic conditions. At last, a short mesh convergence analysis leads to the choice of an average element size of 100 mm.

In all the cases addressed thereafter, the order of appearance of the buckling modes is the same whether one considers the analytical solutions or the

Table 1: Cylindrical shell - Geometric parameters

Length L	5 m
Radius R	2.5 m
Thickness t	25 mm

Table 2: Cylindrical shell - Elastic material properties

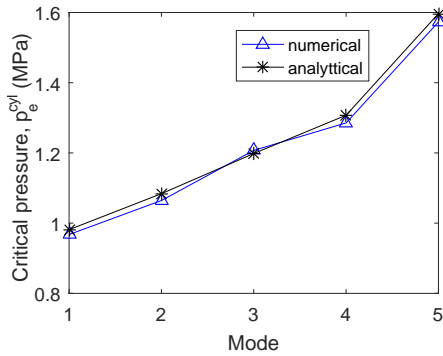
Young's modulus E	200000 MPa
Poisson's ratio ν	0.3

numerical results. It means that the corresponding wave numbers perfectly coincide between the two approaches, especially when focusing on the first buckling mode. In both loading cases (with or without axial compression), whether in elasticity or plasticity, it turns out that the longitudinal half-wave number m minimizing the critical pressure is always equal to 1. Conversely, the circumferential wave number n giving rise to the minimum pressure depends on the material and above all geometric parameters. Dealing now with the buckling pressures, the first five critical values are listed in Table 3, both those derived from the analytical calculations and through the numerical linearized buckling analyses, with and without the pressure end thrust. All the results are shown to be in very good accordance, with a maximum relative error of 2%. It means that the single solution derived through the use of the shallow shell theory turns out to match better with the numerical results obtained in the present case of a follower pressure.

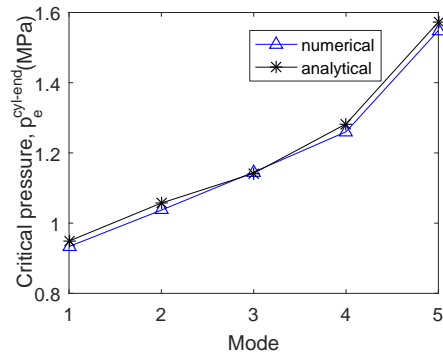
Moreover, in this particular case, the results obtained with the model including the axial compression only slightly differ from the ones obtained with the external pressure alone. More generally, in elasticity, it can be checked that the pressure end thrust will never affect the order of appearance of the buckling modes. The analytical and numerical critical pressures are also compared for the same first five modes in Figures 6(a) and 6(b), considering the case without or with axial compression, respectively. For illustration purposes, Figure 7 shows the first buckling mode of the cylinder under external pressure and axial compression.

Table 3: Cylindrical shell - comparison between analytical and numerical critical values in elasticity

Mode	Analytical (elastic)		FE (linearized)		Relative error	
	p_e^{cyl}	$p_e^{cyl-end}$	p_{e-num}^{cyl}	$p_{e-num}^{cyl-end}$	$\frac{p_e^{cyl} - p_{e-num}^{cyl}}{p_e^{cyl}}$	$\frac{p_e^{cyl-end} - p_{e-num}^{cyl-end}}{p_e^{cyl-end}}$
	(MPa)	(MPa)	(MPa)	(MPa)	(%)	(%)
1	0.9814	0.9488	0.9675	0.9337	1.42	1.59
2	1.0839	1.0572	1.0644	1.0373	1.80	1.88
3	1.1983	1.1419	1.2072	1.1457	-0.74	-0.33
4	1.3073	1.2826	1.2855	1.2606	1.67	1.72
5	1.5968	1.5728	1.5730	1.5491	1.49	1.51



(a)



(b)

Figure 6: Cylindrical shell - analytical and numerical critical pressures for the first five modes in elasticity: (a) under external pressure only; (b) including pressure end thrust

In Figure 8, the first (minimum) critical pressure is plotted for various length-to-radius ratios, still comparing analytical and numerical results in both loading cases (in practice, the radius is kept constant and the length is varied). The corresponding values are also listed in Table 4. All the results are shown again to be in very good accordance, with a relative error of 3% at the maximum. Moreover, the comparison between the analytical values with and without axial compression (last column of Table 4) shows a major

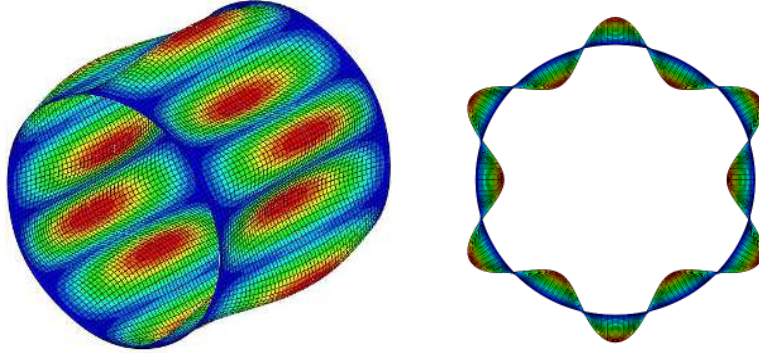


Figure 7: Cylindrical shell under external pressure and axial compression: first buckling mode in elasticity ($n=6$, $m=1$, $p_{e-num}^{cyl-end}=0.9337$ (MPa))

influence of the pressure end thrust for particularly short cylinders, whereas it hardly affects the critical value for sufficiently long cylinders. All these results confirm the validity of the analytical solutions (27) and (31) for a wide length range.

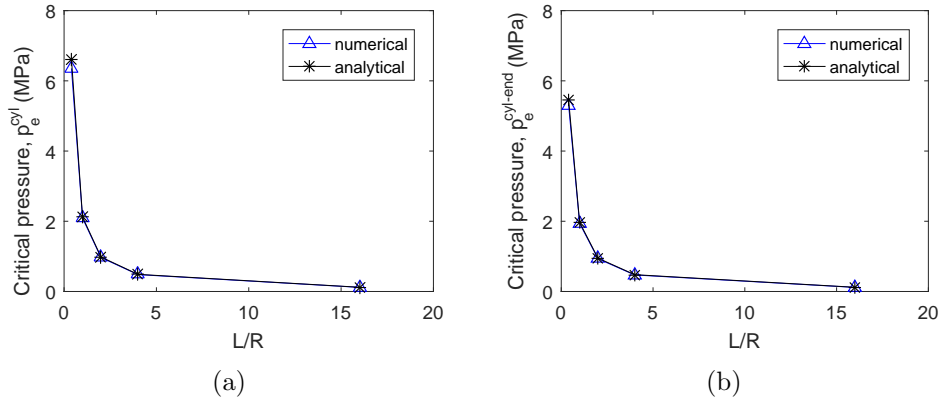


Figure 8: Cylindrical shell - analytical and numerical first critical pressures in elasticity vs. the length-to-radius ratio: (a) under external pressure only; (b) including pressure end thrust

Next, incremental computations have been performed in plasticity, so as to validate the plastic buckling results. In the present case of a cylindrical shell, imperfections need to be introduced so as to trigger the buckling phenomenon. The axial compression is first disregarded. In such conditions, it can be shown that the order of appearance of the first buckling modes in

Table 4: Cylindrical shell - comparison between analytical and numerical first critical values in elasticity for various length-to-radius ratios

L/R	Analytical (elastic)		FE (linearized)		Relative error		Influence of the pressure end thrust
	p_e^{cyl}	$p_e^{cyl-end}$	p_e^{cyl}	$p_e^{cyl-end}$	$\frac{p_e^{cyl} - p_e^{cyl-num}}{p_e^{cyl}}$	$\frac{p_e^{cyl-end} - p_e^{cyl-end-num}}{p_e^{cyl-end}}$	
	(MPa)	(MPa)	(MPa)	(MPa)	(%)	(%)	(%)
0.4	6.6133	5.4604	6.3814	5.3084	3.51	2.78	17.4
1	2.1194	1.9676	2.0903	1.9389	1.37	1.46	7.2
2	0.9814	0.9488	0.9675	0.9337	1.42	1.59	3.3
4	0.4883	0.4790	0.4813	0.4709	1.43	1.69	1.9
16	0.1202	0.1196	0.1172	0.1162	2.50	2.84	0.5

plasticity, as determined analytically, is the same as that obtained in elasticity through finite element linearized buckling analyses, as seen in Table 5. The first mode in plasticity is notably the first mode already obtained in elasticity, which will be thus employed as the initial imperfection shape in the incremental calculations. A new geometry has been considered in plasticity and a tangent modulus has been added to the model, which are all specified in Table 5.

Figure 9 represents a typical force-displacement equilibrium curve obtained through an incremental finite element calculation, involving the appropriate modal imperfection. More precisely, the external pressure is plotted versus the maximum amplitude of displacement throughout the shell. This curve reveals first a linear elastic part, followed by a plastic part (after the plastic threshold). Then the shell bifurcates to a post-buckled shape at a critical point which is immediately followed by a limit point, which will be thus identified as the (first) bifurcation point for comparison with analytical values. Let us mention that the initial yield stress σ_0 should be taken not too far away from the critical point in order to avoid large pre-critical deformations (consistently with the theoretical assumptions). In practice, σ_0 is assigned a value of 95% of the critical (von Mises) stress. Two post-critical deformation shapes have also been added in Figure 9, one just immediately after the bifurcation point (namely at the limit point) and the other one at the end of the computation. The former corresponds roughly to the bifurcation mode (displaying $n=7$ circumferential waves) and the latter to an

Table 5: Cylindrical shell - comparison between elastic and plastic buckling modes ($L=2.5$ m, $R=2.5$ m, $t=50$ mm, $H=2000$ MPa)

Mode	External pressure				External pressure & axial compression			
	FE (linearized)		Analytical (plastic)		FE (linearized)		Analytical (plastic)	
	p_{e-num}^{cyl} (MPa)	$n (m = 1)$	p_p^{cyl} (MPa)	$n (m = 1)$	$p_{e-num}^{cyl-end}$ (MPa)	$n (m = 1)$	$p_p^{cyl-end}$ (MPa)	$n (m = 1)$
1	12.246	7	5.7748	7	11.123	7	2.3838	12
2	13.101	8	6.0437	8	11.780	6	2.3893	11
3	13.441	6	6.3279	6	12.179	8	2.3974	13
4	14.914	9	6.5486	9	14.087	9	2.4222	10
5	17.228	10	7.1786	10	16.516	10	2.4245	14
6	20.064	11	7.9032	11	16.627	5	2.4617	15
7	20.124	5	8.7113	12	19.331	11	2.4948	9
8	23.171	12	9.5982	13	22.468	12	2.5066	16

advanced post-critical state revealing a localization of the deformation.

Let us now consider the case of a cylinder under external pressure and axial compression. It can be seen in Table 5 that the buckling modes in plasticity are still generally the same as in elasticity, but not necessarily with the same order of appearance. A particular attention must be thus paid to the choice of the imperfection shape, which must correspond ideally to the first mode in plasticity so as to trigger the proper buckling phenomenon. As an example, with the parameters considered in Table 5, one must retain the eighth elastic mode (still derived from a linearized buckling analysis) for the definition of the imperfection shape, as it corresponds to the first mode in plasticity with a wave number of 12.

Figure 10 displays again a typical equilibrium curve, namely the external pressure versus the maximum displacement amplitude, in the case where the pressure end thrust is taken into account. The post-critical deformed shapes at the maximum pressure and at the end of the computation are also shown in the same figure. At the critical point, the deformation of the shell is shown to be consistent with the first analytical mode, since the wave number in the circumferential direction is the same ($n=12$).

In both cases (with or without axial compression), analytical and numerical critical values are compared to each other. As seen in Table 6, the results

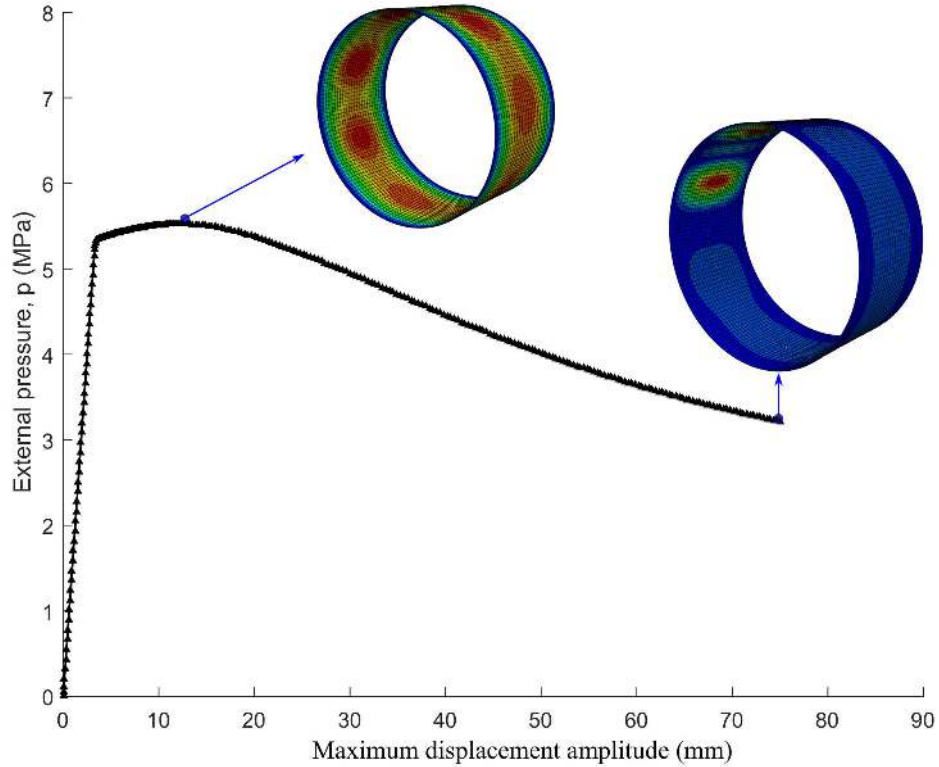


Figure 9: Non-linear buckling analysis of a cylindrical shell under external pressure

are again in very good accordance, for various hardening moduli H .

Lastly, one focuses on the influence of the pressure end thrust. In plasticity, this influence turns out to be much more significant as in elasticity. Figure 11 displays the typical evolutions of the critical values in plasticity, with or without axial compression, according to the circumferential wave number n , provided by Equations (32) and (28), respectively (the nominal value of hardening modulus $H=2000$ MPa has been considered again). It is shown that the pressure end thrust significantly lowers the critical values and even gives rise to a critical value that hardly depends on the wave number, from a certain rank, as if there were many quasi-multiple modes. As a consequence, the order of appearance of the buckling modes is modified when taking into account the pressure end thrust in plasticity.

Finally, for comparison purposes, Figure 12 brings together the illustra-

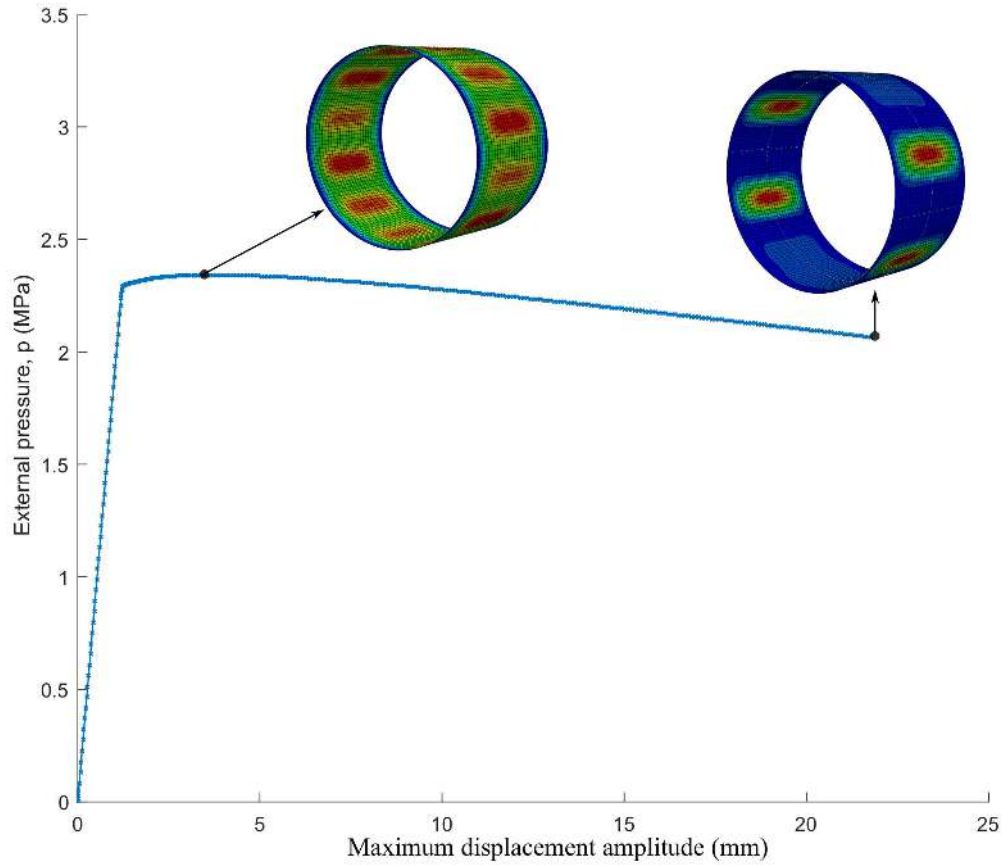


Figure 10: Non-linear buckling analysis of a cylindrical shell under external pressure and axial compression

tion of the influence of the pressure end thrust in both elasticity and plasticity, by plotting the ratio between the first critical pressures with and without axial compression for a large range of length-to-radius ratios. As mentioned above, in elasticity, the additional axial compression only changes the critical values of relatively short cylinders and to a small extent. By contrast, in plasticity, its effect becomes more and more important when the cylinder lengthens and, in any case, the critical value is strongly reduced (at least twice) in presence of axial compression, whatever the length. This strong influence of a transverse compressive stress on the plastic buckling of a shell

Table 6: Cylindrical shell - comparison between analytical and numerical first critical values in plasticity for various hardening moduli

H	External pressure			External pressure & axial compression		
	FE p_{p-num}^{cyl} (MPa)	Analytical (plastic) p_p^{cyl} (MPa)	Relative error $\frac{p_p^{cyl} - p_{p-num}^{cyl}}{p_p^{cyl}}$ %	FE $p_{p-num}^{cyl-end}$ (MPa)	Analytical (plastic) $p_p^{cyl-end}$ (MPa)	Relative error $\frac{p_p^{cyl-end} - p_{p-num}^{cyl-end}}{p_p^{cyl-end}}$ %
4000	5.8078	6.0624	4.20	2.5889	2.6208	1.22
2000	5.5229	5.7748	4.36	2.3418	2.3838	1.76
1000	5.4991	5.6035	1.86	2.1942	2.2400	2.04

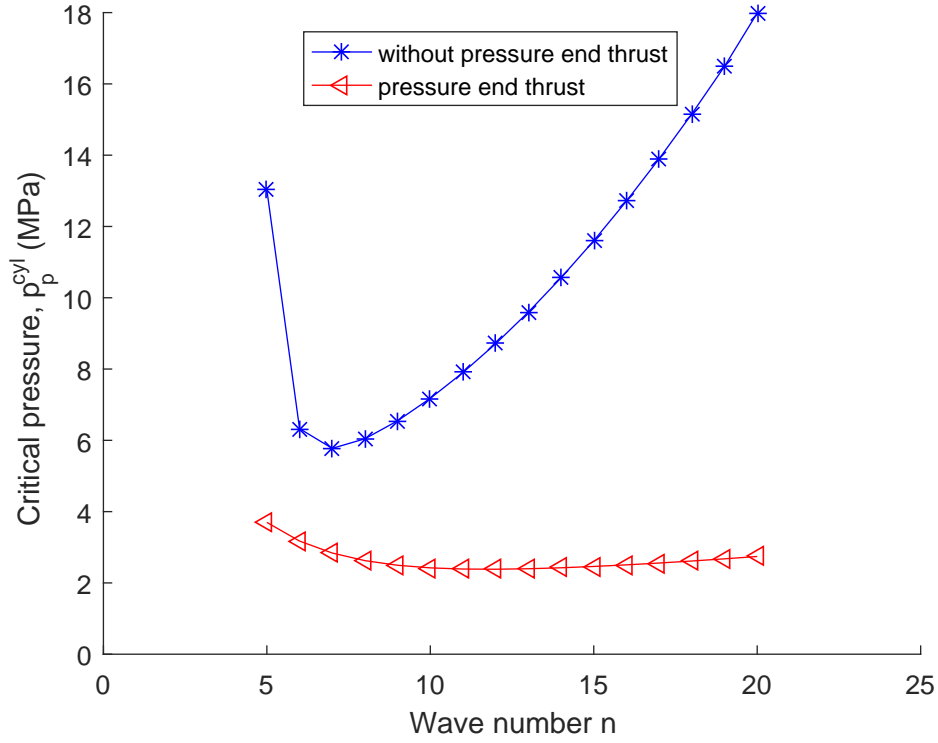


Figure 11: Cylindrical shell - critical pressures in plasticity, with and without axial compression, vs. the circumferential wave number

initially loaded by a uniaxial compressive stress was already observed in [42] in the case of rectangular plates.

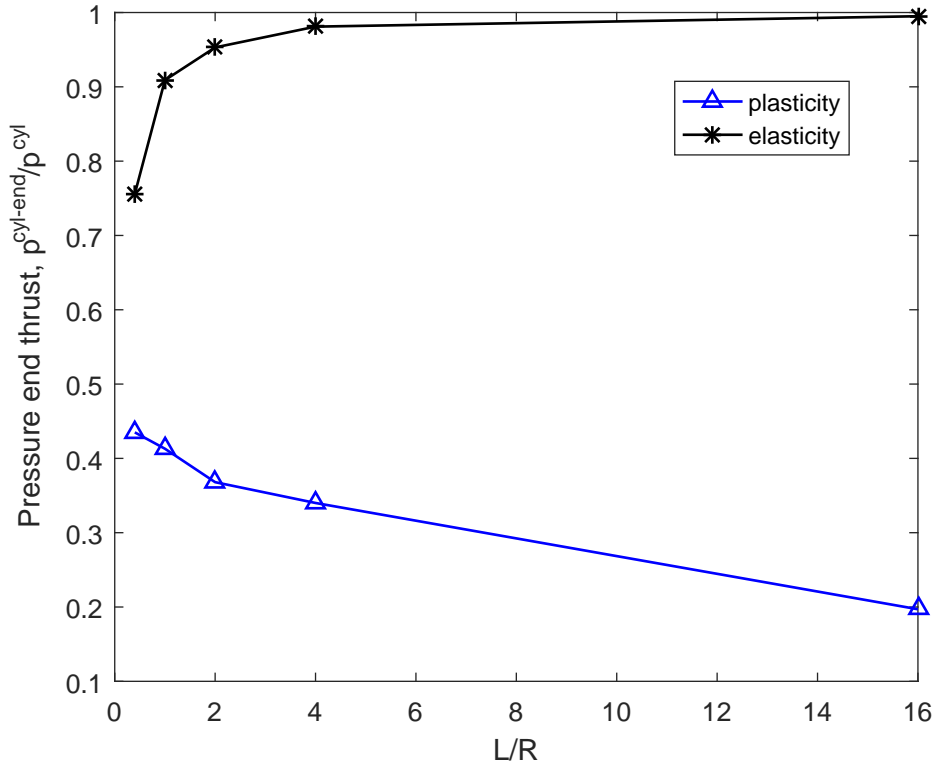


Figure 12: Cylindrical shell - influence of the pressure end thrust on the first critical pressure in elasticity and plasticity vs. the length-to-radius ratio ($R=2.5$ m, $t=50$ mm, $H=2000$ MPa)

4.3. Spherical shells

Dealing now with spherical shells, elastic linearized buckling analyses are first performed using Abaqus software so as to validate the closed-form expression (40) in elasticity. Only one eighth of the total sphere is modeled so as to reduce the computation times (it will be shown that it does not prevent us from obtaining all the sought buckling modes). The geometric parameters and elastic material properties are summarized in Table 7. A regular quadrangular mesh has been retained so as to prevent from singularity problems

(see Figure 13(a)). In the present case of a spherical shell, it is well-known (at least in elasticity) that the critical pressure does not depend on the dead or follower nature of the applied pressure. However, a follower external pressure is retained, for consistency purposes. A short mesh convergence analysis leads to the choice of an element size of about 20 mm.

Table 7: Spherical shell - Material and geometric parameters

Young's modulus E	200000 MPa
Poisson's ratio ν	0.3
Radius R	500 mm
Thickness t	5 mm

In this particular problem, due to the spherical symmetry of the geometry and loading, it appears that the first modes (up to a very high rank) all display almost the same critical pressure, as seen in Figure 13(b-f). The presence of such multiple modes has already been emphasized during the theoretical analysis, since it was proved that the critical pressure was only dependent on the sum of the squares of the wave numbers, in such a way that many pairs of wave numbers (namely many buckling modes) correspond to the same critical values, especially to the minimum one. The order of appearance of the buckling modes will thus highly depend on the mesh refinement.

The analytical minimum critical value (40) is then compared to its numerical counterpart for various radius-to-thickness ratios in Table 8 (the thickness is varied while the radius is kept constant). The maximum relative error is less than 2%.

Last, incremental calculations are performed so as to validate the closed-form expression of the critical pressure in plasticity (38). A corresponding equilibrium curve is plotted in Figure 14 with the specified geometry and hardening modulus. In plasticity, the first buckling modes are again associated to a unique critical value, so that the choice of the imperfection shape among all these buckling modes would have no particular influence on the results, at least on the maximum admissible pressure (the first mode obtained in elasticity could be arbitrarily retained). In practice, the problem of a spherical shell under external pressure is known to be very imperfection-sensitive. For this reason, the intrinsic imperfection due to the geometric

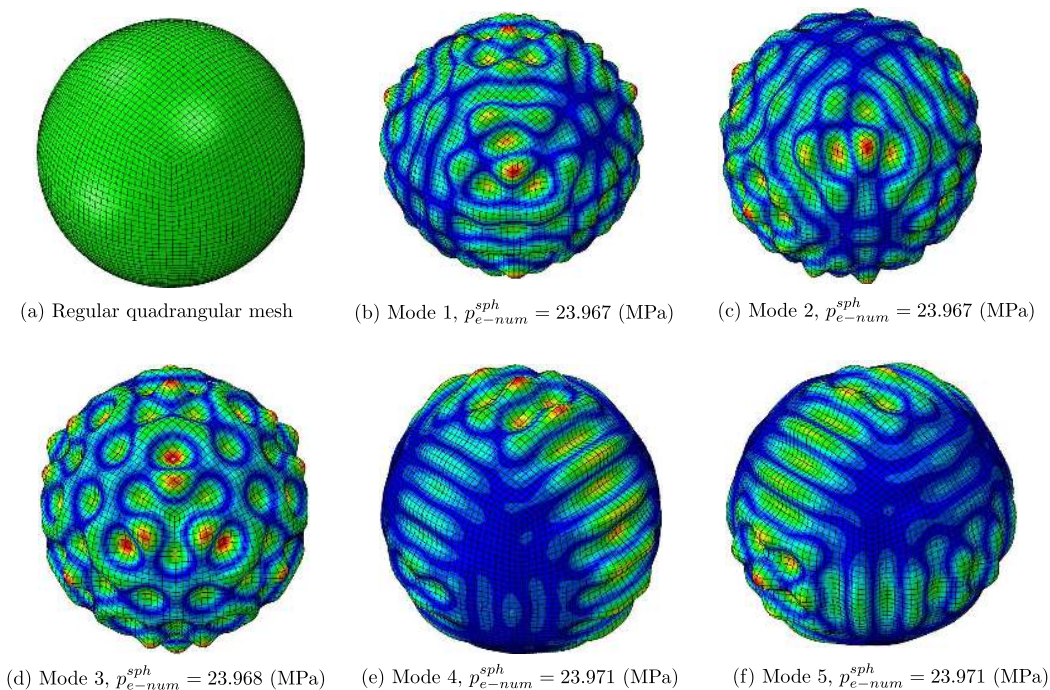


Figure 13: Spherical shell under external pressure: structured mesh and first buckling modes in elasticity

Table 8: Spherical shell - comparison between analytical and numerical first critical values in elasticity for various radius-to-thickness ratios

R/t	FE (linearized)	Analytical (elastic)	Relative error
	p_{e-num}^{sph} (MPa)	p_e^{sph} (MPa)	$\frac{p_e^{sph} - p_{e-num}^{sph}}{p_e^{sph}}$ (%)
50	94.966	94.836	1.93
100	23.967	24.209	1.00
200	6.0378	6.0523	0.24
500	0.9688	0.9684	-0.04

discretization of the surface is sufficient to trigger the buckling phenomenon, and it is not necessary to introduce an additional geometric imperfection into the numerical model.

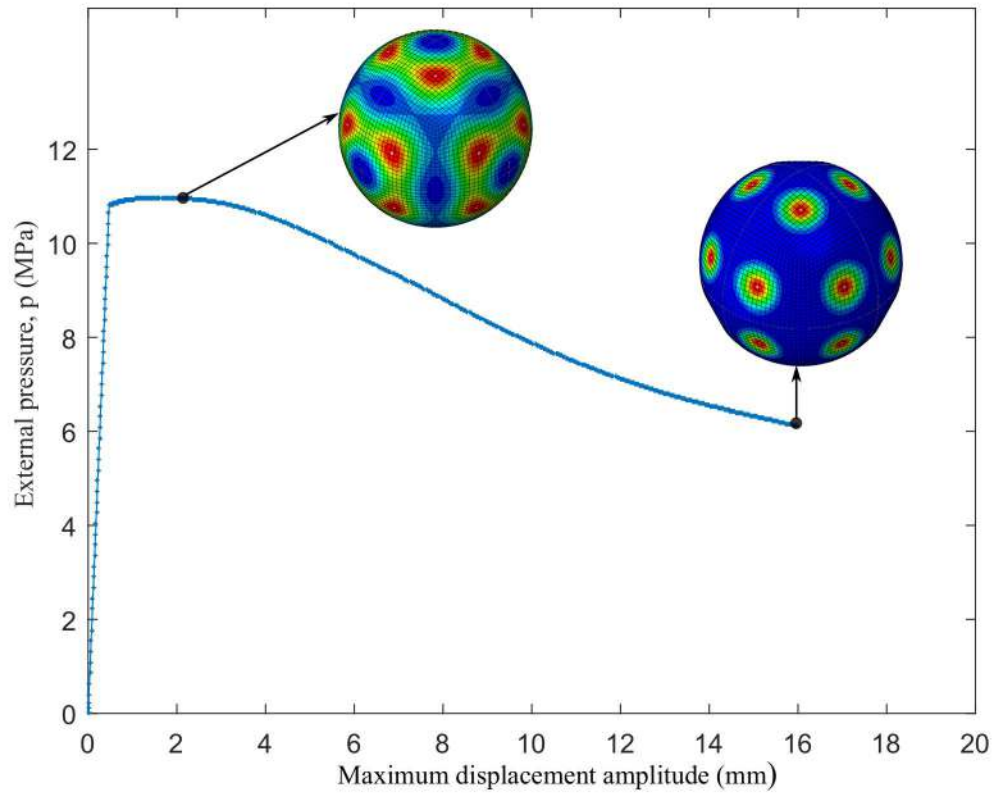


Figure 14: Non-linear buckling analysis of a spherical shell under external pressure ($R=500$ mm, $t=10$ mm, $H=2000$ MPa)

The plastic critical values (both analytical and numerical) are eventually listed in Table 9 for different radius-to-thickness ratios. All the values are again in very good accordance, which definitely validates the theoretical formulation.

5. Comparison with current design codes

This last section aims at comparing the previous closed-form solutions to results stemming from the use of standard design rules. Use will be made of the current methodology implemented in the French CODAP [39] for the buckling design of cylindrical shells, which is mostly derived from the ASME

Table 9: Spherical shell - comparison between analytical and numerical first critical values in plasticity for various radius-to-thickness ratios

R/t	FE	Analytical (plastic)	Relative error
	p_{p-num}^{sph} (MPa)	p_p^{sph} (MPa)	$\frac{p_p^{sph} - p_{p-num}^{sph}}{p_p^{sph}}$ (%)
50	10.9711	11.3785	3.58
100	2.7336	2.8446	3.90
200	0.6853	0.7112	3.64

Boiler and Pressure Vessel Code (BPVC) [38]. First, the calculation procedure will be briefly described (interested readers may find a complete presentation of the method and its demonstration in [52]). Then, numerical applications will be performed for various geometries, so as to confront the results obtained by the current design rules and the previous closed-form solutions.

In a few words, in the French CODAP, the critical external pressure of an elastic cylindrical shell, accounting for the pressure end thrust, is classically obtained through the following formula:

$$p_c = KE \left(\frac{t}{D_o} \right)^3 \quad (41)$$

where the coefficient K is supposed to depend only on the geometric characteristics of the shell, namely the length L , thickness t and outside diameter D_o of the cylinder. Based on this, the critical circumferential stress can be deduced:

$$\Sigma_{\theta\theta}^c = p_c \frac{R}{t} = KE \left(\frac{t}{D_o} \right)^3 \frac{R}{t} \approx \frac{KE}{2} \left(\frac{t}{D_o} \right)^2 \quad (42)$$

and a pseudo-strain is evaluated as follows:

$$A = \frac{\Sigma_{\theta\theta}^c}{E} \approx \frac{K}{2} \left(\frac{t}{D_o} \right)^2 \quad (43)$$

This critical strain value A also depends only on the geometric parameters, and it is determined in practice by using abacuses C4.2.9.1 [39]. From

this numerical value and Young’s modulus, the critical pressure can be obtained in a straightforward way, as soon as elasticity is concerned.

In the more general case of elastic-plastic buckling, a stress-strain curve like the one displayed in Figure 15 is used so as to estimate a stress parameter B . This curve results from an experimental uniaxial tensile test and applies to carbon or low-alloy steels, within a particular temperature range. The elastoplastic buckling pressure writes then:

$$p_{c-codap}^{cyl-end} = \frac{4B}{D_o/t} \quad (44)$$

It can be checked that this expression gives naturally the same value in elasticity as obtained by using directly Equations (41) and (43) (since the linear elastic part of the stress-strain curve in Figure 15 satisfies actually the equation $B = EA/2$). Finally, let us mention that, in practice, a knock-down factor of 3 is then usually applied for design purposes.

In the sequel, a cylindrical shell of given length and radius is considered. By varying the thickness, four cases are considered, represented by the four numbered crosses on the stress-strain curve in Figure 15. In the first two cases (1) and (2), the cylindrical shell is sufficiently thin so that the representative point in the stress-strain curve belongs to the elastic part and the buckling response is elastic. Conversely, the last two cases (3) and (4) correspond to thicker cylindrical shells for which plastic buckling is expected, given the position of the associated points on the behavior curve. The critical pressures obtained through Equation (44) (without knock-down factors) are compared to the analytical solutions previously derived, namely using Equations (31) in elasticity and (32) in plasticity, respectively. The Young’s modulus and tangent modulus involved in these equations are deduced from the stress-strain curve of Figure 15, the latter depending on the slope of the curve at the representative point in case of plasticity. All the critical pressures are listed in Table 10 and the ratio between the value from the standard and the corresponding analytical value is added for clarity purposes.

First, in elasticity, apart from the use of a safety factor, the present analytical solutions agree perfectly with the values provided by the CODAP/ASME standard. In contrast, in the case of plasticity, the analytical critical pressure is found to be equal to 75% on average of the corresponding value recommended by the standard (this ratio of about 0.75 has also been obtained in other configurations, by varying the length of the cylindrical shell). The present work therefore shows, through these illustrative examples, that the

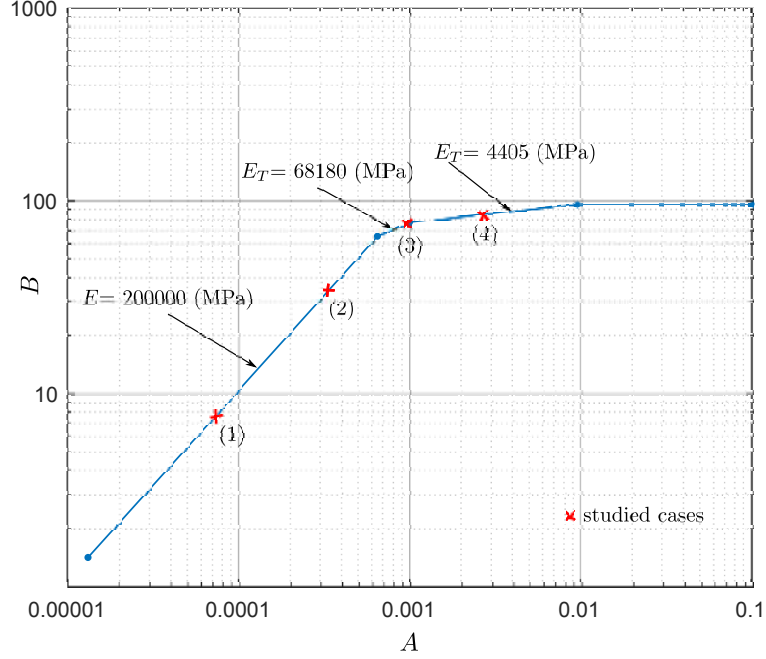


Figure 15: Stress-strain curve used for the determination of the elastic-plastic buckling pressures of cylindrical tubes under external pressure (accounting for pressure end thrust) made of carbon or low-alloy steels under a temperature $T < 150^\circ\text{C}$ [39]

Table 10: Cylindrical shell - comparison between the proposed closed-form solutions and the French CODAP ($R=500$ mm, $L=500$ mm)

Cases	R/t	French CODAP				Analytical		Relative ratio $\frac{p_c^{cyl-end}}{p_{c-codap}^{cyl-end}}$
		A	B (MPa)	$p_{e-codap}^{cyl-end}$ (MPa)	$p_{p-codap}^{cyl-end}$ (MPa)	$p_e^{cyl-end}$ (MPa)	$p_p^{cyl-end}$ (MPa)	
(1)	500	0.0000819	8.489	0.03392	–	0.03395	–	1.001
(2)	200	0.000337	34.117	0.34032	–	0.34030	–	1.000
(3)	100	0.000967	75.993	–	1.5123	–	1.1067	0.732
(4)	50	0.002670	84.620	–	3.3513	–	2.6758	0.798

current procedure in plastic buckling analysis is possibly not so conservative as expected.

6. Conclusions

In this paper, the elastoplastic buckling problem of a shell under external pressure has been investigated. A general approach has been defined, based on the 3D bifurcation theory. The critical pressures and the associated buckling modes are obtained by solving the so-called bifurcation equation, which has proven to be successful in addressing many other buckling problems with various geometries, loading conditions and constitutive laws. In the present case, the classical bifurcation equation (conventionally used for conservative problems) has been slightly modified so as to take into account the follower nature of the external pressure. Next, the general choice was made of the shallow shell theory to express the kinematics of the shells further considered, in order to simplify at best the governing equations of the future problems.

This general formulation is then applied to the particular cases of a cylindrical and spherical shell. These two geometries are the most frequently encountered in practical pressure equipments, and are also simple enough to hope for explicit solutions. In the case of a cylindrical shell, axial compression is added in a second step so as to take into account the pressure end thrust. In all cases, closed-form analytical solutions are established. While elastic critical values are mostly well-known for these particular problems, the plastic buckling pressures are supposedly original. For validation purposes, numerical finite element computations are performed, namely linearized buckling analyses in elasticity and incremental calculations in plasticity. As soon as the buckling phenomenon occurs within the context of small pre-critical transformations, the analytical and numerical results are found to be in very good agreement. By the way, these formulae have enabled us to analyze efficiently the main features of the buckling phenomena of such shell structures under external pressure, focusing naturally on the first critical value. It was shown in particular that the occurrence of plasticity before buckling modifies considerably the nature of the response and thus the collapse mode of the structure. Not only the critical value is much lower in plasticity than in elasticity, but also the buckling mode (identified here by a particular wave number) can strongly change between the two cases. Also, the pressure end thrust, which is traditionally known to be virtually not influential in the elastic buckling of cylindrical shells under pressure, plays a major role in

plasticity, where it reduces the critical value by a factor of about 2 to 5, depending on the geometry of the cylinder.

In the end, this general formulation is shown to give satisfactory results in the two cases of cylindrical and spherical shells. The new expressions derived in plasticity enable one to extend rigorously the validity domain of classical elastic critical values to moderately thick shells, for which plasticity is expected to occur before instability. All these analytical simple formulae constitute interesting reference expressions for dimensioning purposes. In some cases, when plasticity is involved, they are found to be more conservative than the current design rules, and could thus serve as a basis for a new formulation of such procedures. In all cases, they correspond to the idealized context of perfect structures with simple boundary conditions, on the basis of which one may build some more practical rules, including the influence of imperfections or other perturbations. All of this motivates us to apply the same formulation to new geometries and/or under other (possibly combined) loading conditions, by using approximate solution methods, if necessary in the case of more complex configurations. From all these results, a practical tool is likely to be developed, only based on such analytical solutions, for the purpose of designing pressure equipments as a whole against elastic/plastic buckling.

References

- [1] G. H. Bryan, Application of the energy test to the collapse of a long thin pipe under external pressure, in: Proceedings of the Cambridge Philosophical Society, vol. VI, 1889.
- [2] V. N. Paimushin, Static and dynamic beam forms of the loss of stability of a long orthotropic cylindrical shell under external pressure, *Journal of Applied Mathematics and Mechanics* 72 (6) (2008) 738–747.
- [3] J. Xue, Local buckling in infinitely, long cylindrical shells subjected uniform external pressure, *Thin-Walled Structures* 53 (2012) 211–216.
- [4] S. Salahshour, F. Fallah, Elastic collapse of thin long cylindrical shells under external pressure, *Thin-Walled Structures* 124 (2018) 81–87.
- [5] R. V. Southwell, On the collapse of tubes by external pressure, *Philosophical Magazine* 29 (6) (1915) 67–77.

- [6] N. Yamaki, *Elastic Stability of Circular Cylindrical Shells*, North-Holland Press, 1984.
- [7] E. I. Grigolyuk, V. V. Kabanov, *Stability of Shells*, Nauka, 1978.
- [8] G. Papadakis, Buckling of thick cylindrical shells under external pressure: A new analytical expression for the critical load and comparison with elasticity solutions, *International Journal of Solids and Structures* 45 (20) (2008) 5308–5321.
- [9] H. L. T. Nguyen, I. Elishakoff, V. T. Nguyen, Buckling under the external pressure of cylindrical shells with variable thickness, *International Journal of Solids and Structures* 46 (24) (2009) 4163–4168.
- [10] C. Basaglia, D. Camotim, N. Silvestre, GBT-based buckling analysis of steel cylindrical shells under combinations of compression and external pressure, *Thin-Walled Structures* 144 (2019) 106274.
- [11] R. Zoelly, *Über ein Knickungsproblem an der Kugelschale*, Ph.D. thesis, ETH Zürich, 1915.
- [12] J. W. Hutchinson, Imperfection sensitivity of externally pressurized spherical shells, *Journal of Applied Mechanics* 34 (1) (1967) 49–55.
- [13] J. W. Hutchinson, Buckling of spherical shells revisited, *Proceedings of the Royal Society A: Mathematical, Physical and Engineering Sciences* 472 (2016) 20160577.
- [14] S. Palusamy, N. C. Lind, A consistent theory for spherical shells in equilibrium, *Nuclear Engineering and Design* 21 (3) (1972) 350–357.
- [15] M. Sato, M. A. Wadee, K. Iiboshi, T. Sekizawa, H. Shima, Buckling patterns of complete spherical shells filled with an elastic medium under external pressure, *International Journal of Mechanical Sciences* 59 (1) (2012) 22–30.
- [16] S. N. Krivoshapko, Research on general and axisymmetric ellipsoidal shells used as domes, pressure vessels, and tanks, *Applied Mechanics Reviews* 60 (6) (2007) 336–355.
- [17] Y. Q. Ma, C. M. Wang, K. K. Ang, Buckling of super ellipsoidal shells under uniform pressure, *Thin-Walled Structures* 46 (6) (2008) 584–591.

- [18] V. Barathan, V. Rajamohan, Nonlinear buckling analysis of a semi-elliptical dome: Numerical and experimental investigations, *Thin-Walled Structures* 171 (2022) 108708.
- [19] H. Sharghi, M. Shakouri, M. A. Kouchakzadeh, An analytical approach for buckling analysis of generally laminated conical shells under axial compression, *Acta Mechanica* 227 (4) (2016) 1181–1198.
- [20] Y. Chung, Buckling of composite conical shells under combined axial compression, external pressure, and bending, Ph.D. thesis, New Jersey Institute of Technology, 2001.
- [21] F. R. Shanley, Inelastic column theory, *International Journal of Aeronautical Sciences* 14 (1947) 261–267.
- [22] J. Becque, The application of plastic flow theory to inelastic column buckling, *International Journal of Mechanical Sciences* 111-112 (2016) 116–124.
- [23] P. Seide, E. Z. Stowell, Elastic and plastic buckling of simply supported solid-core sandwich plates in compression, NACA Report 967, 1950.
- [24] A. Cimetière, Sur la modélisation et le flambage des plaques élastoplastiques, Ph.D. thesis, University of Poitiers, 1987.
- [25] S. C. Batterman, Plastic buckling of axially compressed cylindrical shells, *AIAA Journal* 3 (2) (1965) 316–325.
- [26] S. C. Batterman, Free-edge plastic buckling of axially compressed cylindrical shells, *Journal of Applied Mechanics* 35 (1968) 73–79.
- [27] J. Chakrabarty, On the problem of uniqueness under pressure loading, *Zeitschrift für Angewandte Mathematik und Physik* 20 (5) (1969) 696–706.
- [28] J. Chakrabarty, Plastic buckling of cylindrical shells subjected to external fluid pressure, *Zeitschrift für Angewandte Mathematik und Physik* 24 (2) (1973) 270–280.
- [29] M. Takla, Insight into elastic–plastic bifurcation of pressurized cylinders: Transition between bulging and necking, the line of catastrophic failure, *International Journal of Mechanical Sciences* 148 (2018) 73–83.

- [30] M. Takla, Instability and axisymmetric bifurcation of elastic-plastic thick-walled cylindrical pressure vessels, *International Journal of Pressure Vessels and Piping* 159 (2018) 73–83.
- [31] M. Takla, Bifurcation of elastic–plastic thick-walled cylindrical structures, *International Journal of Mechanical Sciences* 141 (2018) 303–315.
- [32] M. Takla, Non-symmetric bifurcation and collapse of elastic-plastic thick-walled cylinders under combined radial and axial loading, *Marine Structures* 64 (2019) 246–262.
- [33] Y. Zhu, Y. Dai, Q. Ma, W. Tang, Buckling of externally pressurized cylindrical shell: A comparison of theoretical and experimental data, *Thin-Walled Structures* 129 (2018) 309–316.
- [34] J. W. Hutchinson, Plastic buckling, *Advances in Applied Mechanics* 14 (1974) 67–144.
- [35] B. Liu, FE analysis of plastic buckling of plates with initial imperfections and simulation of experiments, Ph.D. thesis, McGill University, Montreal, 2007.
- [36] E. Ore, D. Durban, Elastoplastic buckling of axially compressed circular cylindrical shells, *International Journal of Mechanical Sciences* 34 (9) (1992) 727–742.
- [37] K. W. Neale, Effect of imperfections on the plastic buckling of rectangular plates, *Journal of Applied Mechanics* 42 (1) (1975) 115–120.
- [38] ASME, American Society of Mechanical Engineers – Boiler and Pressure Vessel Code, Section A-4, 2007.
- [39] CODAP, French Pressure Vessel Code, Sections C-4 and C-10, 2020.
- [40] J. M. Rotter, H. Schmidt, Buckling of steel shells: European design recommendations, in: *European Convention for Constructional Steel Works*, 2008.
- [41] M. Tall, S. Hariri, P. Le Grogneq, Y. Simonet, Elastoplastic buckling and collapse of spherical shells under combined loadings, *Thin-Walled Structures* 123 (2018) 114–125.

- [42] P. Le Grogneq, A. Le van, Some new analytical results for plastic buckling and initial post-buckling of plates and cylinders under uniform compression, *Thin-Walled Structures* 47 (8-9) (2009) 879–889.
- [43] P. Germain, Q. S. Nguyen, P. Suquet, Continuum thermodynamics, *Journal of Applied Mechanics* 50 (1983) 1010–1020.
- [44] B. Halphen, Q. S. Nguyen, Sur les matériaux standard généralisés, *Journal de Mécanique* 14 (1) (1975) 39–63.
- [45] A. E. Green, P. M. Naghdi, A general theory of an elastic-plastic continuum, *Archive for Rational Mechanics and Analysis* 18 (1965) 251–281.
- [46] A. E. Green, P. M. Naghdi, Some remarks on elastic-plastic deformation at finite strain, *International Journal of Engineering Science* 9 (12) (1971) 1219–1229.
- [47] J. W. Hutchinson, On the postbuckling behavior of imperfection-sensitive structures in the plastic range, *Journal of Applied Mechanics* 39 (1) (1972) 155–162.
- [48] Q. S. Nguyen, *Stability and Nonlinear Solid Mechanics*, Wiley, 2000.
- [49] V. N. Paimushin, The equations of the geometrically non-linear theory of elasticity and momentless shells for arbitrary displacements, *Journal of Applied Mathematics and Mechanics* 72 (5) (2008) 597–610.
- [50] V. N. Paimushin, On the forms of loss of stability of a cylindrical shell under an external side pressure, *Journal of Applied Mathematics and Mechanics* 80 (1) (2016) 65–72.
- [51] A. M. A. van der Heijden, *W.T. Koiter’s Elastic Stability of Solids and Structures*, Cambridge University Press, 2008.
- [52] M. H. Jawad, J. R. Farr, *Structural Analysis and Design of Process Equipment*, Wiley, 2018.